

Historical Trends and Future Projections of Key Performance Parameters in Aircraft Design

Huseyin Acar^{*†}, Maxfield Arnon^{*‡}, Michael Tsai[§], and Gokcin Cinar^{¶||}

Department of Aerospace Engineering, University of Michigan, Ann Arbor, Michigan 48109

This study presents a comprehensive analysis of historical trends and future projections for key performance parameters (KPPs) in commercial turbofan aircraft, focusing on operational empty weight to maximum takeoff weight ratio (OEW/MTOW), thrust-to-weight ratio (T/W), thrust-specific fuel consumption (TSFC), and lift-to-drag ratio (L/D). Leveraging the open-source FAST Aerobase, comprising over 400 commercial airframes and 200 engines, drawn from authoritative sources such as FAA and EASA certifications, along with enhanced regression modeling, this study systematically examines the evolution of each KPP in response to technological advancements, market demands, and regulatory constraints. The analysis reveals that TSFC improvements align closely with technological advances, primarily increases in bypass ratio enabled by core downsizing. Trends in OEW/MTOW and T/W are dominated by market-driven range, size, and regulatory factors rather than pure material or propulsion breakthroughs, which indicates limited room for further improvement without disruptive configurations. Cruise L/D improvements have been primarily enabled by wingtip devices, although they are approaching structural and regulatory limits. This work lays a robust foundation for the open-source Future Aircraft Sizing Tool (FAST), equipping designers with data-driven insights to support early-stage design decisions and providing a transparent resource for understanding the historical and technical drivers of commercial aircraft performance.

Nomenclature

k	=	Growth Rate
\dot{m}_f	=	Fuel mass flow rate
n	=	Load Factor
q	=	Dynamic Pressure

*These authors contributed equally to this work.

†Graduate Student, Department of Aerospace Engineering, University of Michigan, Ann Arbor, Michigan 48109.

‡Graduate Student, Department of Aerospace Engineering, University of Michigan, Ann Arbor, Michigan 48109, AIAA Student Member.

§Research assistant, Department of Aerospace Engineering, University of Michigan, Ann Arbor, Michigan 48109.

¶Assistant Professor, Department of Aerospace Engineering, University of Michigan, Ann Arbor, Michigan 48109, AIAA Senior Member.

||Corresponding author. Email: cinar@umich.edu

AR	=	Aspect Ratio
C	=	Thrust Specific Fuel Consumption
C_{D0}	=	Coefficient of drag at zero lift
C_{DR}	=	Coefficient of additional drags
D	=	Drag
K_1	=	Coefficient in lift-drag polar equation
K_2	=	Coefficient in lift-drag polar equation
L	=	Lift
L/D	=	Lift-to-drag ratio
La	=	Lower Asymptote
M_0	=	Cruise Mach Number
P_s	=	Weight-specific excess power
Q_0	=	Heat of working fluid prior to combustion
Q_f	=	Heat of working fluid after combustion
R	=	Range
Re_{mac}	=	Mean Aerodynamic Chord Reynolds Number
S	=	Wing Area
T	=	Maximum Takeoff Thrust
U	=	Upper Asymptote
V	=	Velocity
V_e	=	(Core) exit velocity
V_∞	=	Freestream velocity
W	=	Weight
W_0	=	Gross weight
W_{Empty}	=	Empty weight
W_f	=	Final weight
W_{Fuel}	=	Fuel weight
W_i	=	Initial weight
$W_{payload}$	=	Payload weight
W/S	=	Wing Loading
α	=	Installed Thrust Lapse
β	=	Instantaneous Weight Fraction

η_p	=	Propulsive Efficiency
η_{therm}	=	Thermal Efficiency
η_{tot}	=	Overall Engine Efficiency
θ	=	Cruise to sea-level temperature ratio
τ	=	Inflection point

I. Introduction

The aviation industry has witnessed significant advancements in aircraft design, driven by evolving technological capabilities and market demands. This paper methodically analyzes historical trends in key performance parameters (KPPs) of aircraft and projects these trends into the future.

Contemporary aircraft design methodologies, as presented in canonical references such as Raymer [1], Roskam [2], and Torenbeek [3], often utilize regressions based on historical data for various aircraft categories. After determining the requirements of the designed aircraft, top-level metrics such as the initial weight fraction and thrust-to-weight ratio are predicted from the parameters of similar aircraft. However, the data underpinning these regressions often lack transparency, accessibility, and clarity in assumptions. For instance, a single aircraft can have multiple weight variations due to different configurations or modifications, yet how such variations are accounted for in the regressions is often ambiguous. Furthermore, these regressions may not capture how these parameters are affected by component-level technological advancements over time.

Several studies have investigated the historical evolution of aircraft performance parameters, though limitations in data transparency and scope are evident. Martinez et al. [4] conducted an extensive analysis using data from 73 jet engines and 116 propeller-driven airplanes to trace the evolution of aircraft performance. Despite the large dataset, this study lacked transparency in data collection and did not clearly address variations in weight. Similarly, Lee [5] examined trends in thrust specific fuel consumption (TSFC), lift-to-drag ratio (L/D), and the operational empty weight to maximum takeoff weight ratio (OEW/MTOW) to assess potential emission reductions in aviation. However, the analysis was limited to 31 aircraft, which may not fully represent historical evolution. Ballal and Zelina [6] extended this investigation to include aeroengine specifications from 1938 to 2003 across both military and civil aircraft, yet the specific engines analyzed were not clearly identified.

A recurring issue in these studies is the lack of direct publication of certain key parameters, such as L/D, by authorized sources, necessitating their estimation through indirect methods. This often leads to inconsistencies in historical analyses. For instance, some studies, like Martinez et al. [7], estimate L/D without detailing the underlying parameters, while others like Lee [5] provide L/D values but fail to cite clear data sources. As a result, Martinez and Perez [8] reported a 50% increase in L/D over time, whereas Lee et al. [5] observed only a 15% improvement,

highlighting the variability in conclusions drawn from different methodologies [9].

The literature also often overlooks the interdependencies between various performance parameters, focusing narrowly on individual metrics. For example, analyzing changes in OEW/MTOW as an indicator of structural efficiency requires considering how aircraft size and range capabilities have evolved. Without acknowledging these interactions, studies may underestimate the impact of advances in materials and composite technologies on structural efficiency.

This study aims to address these limitations by conducting a comprehensive analysis of selected performance parameters across a wide range of aircraft. By providing future projections, this research offers insights that may support further studies on cost and emission reduction strategies in the years ahead. It highlights the necessity of a holistic approach to parameter analysis, demonstrating that a more detailed understanding of the evolution of performance parameters is an essential piece of accurate forecasting and effective design innovation.

This study stands apart by examining a comprehensive and fully transparent database of over 400 aircraft, spanning diverse sizes and entry-into-service (EIS) years. The Aircraft and Engine Registry Open-source dataBASE (Aerobase) [10], constructed from publicly available information from trusted sources such as manufacturer's technical specifications sheets, airport planning manuals (APM), and type certificate data sheets (TCDS) published by the Federal Aviation Administration (FAA) and the European Union Aviation Safety Agency (EASA), offers a wide view of the evolution of aircraft KPPs. By correlating these parameters with underlying physical phenomena, the study aims to provide a more profound understanding of the observed trends.

An important outcome of this research is the development of the Future Aircraft Sizing Tool (FAST) [11], an open-source software that leverages the Aerobase and the historical trends analyzed in this paper. Developed as part of NASA's Electrified Powertrain Flight Demonstrators (EPFD) project, FAST relies on the historical trends and projections of KPPs to generate initial aircraft designs with minimal input, allowing for rapid exploration and estimation. At the same time, it is flexible enough to incorporate physics-based models or more detailed data when available. Although this paper does not detail the construction of FAST, it serves as the foundation for the tool by offering a comprehensive analysis of the historical data that underpins its predictive capabilities.

The insights from this research are intended for aircraft designers and researchers. While rooted in historical data, projecting future trends inherently carries uncertainties. However, with a clear understanding of past trends and their drivers, stakeholders can make informed decisions for future aircraft designs, ensuring alignment with technological progress and market requirements.

Following this introduction, the selection of KPPs, data collection, and historical trend analysis in the technical approach are discussed. The subsequent section provides historical trends, identifies underlying drivers, and makes informed projections for the future.

II. Technical Approach

A. Selection of Key Performance Parameters (KPPs)

Key performance parameters are critical in the early stages of aircraft design, offering a foundational set of variables that dictate performance and sizing. Initially, KPPs are defined as abstract yet essential elements that support high-level aircraft modeling, sizing, and performance assessments. These parameters are selected to provide an appropriate level of abstraction suitable for the conceptual design stage. For example, the Breguet Range Equation (BRE), given in Eq. 1, a cornerstone for estimating aircraft performance, utilizes high-level performance parameters integral to aerodynamic efficiency (through L/D), propulsion system efficiency (through $TSFC$, or in short, C), performance (through V), and the aircraft weight ratio (through W_i/W_f).

$$R = \frac{V}{TSFC \times g} \frac{L}{D} \ln \left(\frac{W_i}{W_f} \right) \quad (1)$$

Despite its simplicity, the BRE is a powerful tool for early-stage analysis because it provides valuable insights with minimal data requirements. However, as the aerospace industry explores disruptive technologies, such as those with electrified propulsion, the traditional BRE faces limitations in accurately estimating performance due to the distinct characteristics of these new propulsion systems. Expanding upon this conventional approach, Jansen and Duffy [12–14] identified and applied new KPPs to extend the BRE to Electrified Aircraft Propulsion (EAP) systems. They introduced modifications that account for the efficiency and weight of the turboelectric drive, allowing for a more nuanced assessment of aircraft performance. Their work categorizes KPPs into parameters that directly correlate with aircraft aerodynamics, structures, propulsion, and *power*—a distinction not separately made in the BRE—laying a foundation for a generalized parameter space that encompasses both conventional and electrified aircraft propulsion concepts. Alternatively, range can be normalized by total energy consumption, so that the energy-specific range of conventional and hybrid concepts can be directly compared (provided that aerodynamic efficiencies are similar). This approach offers insights into the total energy usage, simultaneously acknowledging the benefits of decreasing mass and high propulsive efficiency that conventional and electric concepts take advantage of respectively.

Acknowledging the contributions of several authors who have identified historical trends and future projections in electric powertrain-specific components, this paper fills in the remaining KPPs. Specifically, Pastra et al. [15] explore future projections for the specific power and efficiency of electric machines (EMs) used in aircraft, Hall et al. [16] project the specific power and efficiency of power converters through the year 2050, and Tiede et al. [17] make specific energy projections for electric aircraft

In this study, the focus is predominantly on conventional KPPs—OEW/MTOW, T/W, L/D, and TSFC—due to their significance in representing various facets of aircraft performance: structural efficiency, aerodynamic efficiency, and propulsion efficiency. While the list of KPPs can be expanded, this approach emphasizes the importance of making

informed estimates with a limited set of data, particularly when designing innovative and unconventional aircraft.

B. Data Collection Approach

Historical data serves as a foundational element for forecasting future trends in aircraft and engine KPPs. To ensure reliable projections, a substantial database was required. However, many existing databases often lack source citations and seldom offer the level of specificity needed for the intended analysis. For instance, Roux published two books on turbofan and turboprop engines in 2007 and 2011 respectively [18, 19]. These books are comprehensive, however they only provide information on engines, not aircraft themselves, and do not include contemporary designs. Additionally, the data books are not formatted for easy digital manipulation. Janes *All The World's Aircraft* [20] is a large aircraft database, although it is not free to use. The FAA [21], Eurocontrol [22], and Jenkinson et al. [23] have publicly available databases online, however these are not comprehensive, including small sample sets of aircraft data.

To address these shortcomings, this study initiated the compilation of a specialized database, the “FAST Aerobase,” encompassing over 400 commercial aircraft and more than 200 turbofan engines, supplemented by a selection of turbojet engines. This database integrates aircraft and engine data to delineate a complete profile of each vehicle.

The primary sources for data collection were TCDS published online by the FAA, EASA, the United Kingdom’s Civil Aviation Authority (CAA), and other government aviation authorities. The TCDS data was enriched with information from aircraft manufacturer brochures and websites, airport planning manuals, and manufacturer CAD models. Similarly, engine data was gathered from TCDS and various data handbooks.

C. Data Structure and Analytical Application in FAST

The data used in this study is publicly available within the FAST repository [10] and can be accessed as either structured MATLAB files or spreadsheets to support reproducibility in various programs such as JMP. For streamlined organization and analysis in MATLAB, the data are hierarchically structured as a MATLAB ‘struct’. Each aircraft entry in the Aerobase contains over 100 parameters detailing various aspects of both the vehicle and its engines. In this structure, “leaves” at the endpoints represent specific parameter values, while “branches” categorize these parameters into broader classifications.

This paper sets the foundation for further predictive analysis within the FAST framework by identifying essential physical relationships in the aircraft data. Building on these foundational insights, Arnson et al. [24] later applied probabilistic regressions to the same dataset, incorporating as much design information as possible to improve upon traditional regression models by Raymer, Roskam, and Jenkinson. This paper examines correlations between entry-into-service (EIS) year and parameters such as OEW and T/W, concluding that EIS alone is an unreliable predictor of OEW-to-MTOW ratios due to OEW’s dependence on mission-specific design requirements rather than purely technological advancements. In this context, EIS refers to the first release of a vehicle, whereas if a subsequent

modification is made, the modified version is treated as a new vehicle entirely. By analyzing these trends, the current study establishes the physical relationships that inform which parameters are most relevant in predicting unknown values during the conceptual design phase—insights that have since been used to guide the regression models in Arnson et al.'s work.

D. S-Curve Modeling of Aircraft Performance Evolution

The database was leveraged to analyze the KPPs that represent the structural, aerodynamic, and propulsion efficiency over the years. These KPPs were examined in relation to both entry-into-service dates of the aircraft and other performance parameters, with the aircraft categorized by aisle type to yield more pronounced trends.

To investigate the historical evolution of KPPs and their connection with other aircraft specifications, scatter plots were used for visual analysis. By superimposing regressions (generally linear) over the scatter plots, general trends of the parameters through time and relationships between parameters can be investigated. Figures include the coefficient of determination, R^2 , which is a statistical measure indicating how much of the variation in the dependent variable is explained by the independent variable. R^2 values range from 0 to 1, where values close to 0 suggest that the model does not explain much of the variability in the outcome, while values close to 1 indicate that a large proportion of the variance in the dependent variable is explained by the model. As mentioned earlier, regressions in this context are primarily intended to identify general trends rather than to precisely predict individual outcomes; therefore, relatively low R^2 values (e.g., below 0.5) are acceptable and expected. In addition to regression lines, bivariate normal density ellipses are superimposed over the scatter plots, and correlations between the relevant parameters are observed visually. The bivariate normal density ellipse is the graphical representation of the bivariate normal density function [25]. Ellipses are drawn with a 90% confidence level, meaning there is a 90% chance that data from the distribution will fall within the ellipse. The orientation of this ellipse allows for understanding the strength and direction of the relationship between the parameters. For example, a circular ellipse indicates that there is no strong correlation between the data, whereas more elongated ellipses show that there is a strong correlation between the data. Moreover, the correlation coefficient (Eq. 2), which indicates the strength and direction of the linear relationship between two variables, is calculated and displayed in the graph. The coefficient ranges from -1 (a perfect negative relationship) to 1 (a perfect positive relationship). Bivariate normal density ellipse were obtained from JMP [26].

$$r = \frac{\text{cov}(X, Y)}{\sigma_X \sigma_Y} \quad (2)$$

where:

- $\text{cov}(X, Y)$ is the covariance between the two variables X and Y ,
- σ_X is the standard deviation of X ,

- σ_Y is the standard deviation of Y .

TSFC has significantly evolved over time due to advancements in engine technology, including high bypass ratios, improved thermodynamic cycles, and advanced materials [27]. Consequently, TSFC is considered a critical technological parameter. The remaining KPPs (OEW/MTOW, T/W, L/D) do not evolve directly with technological development. Instead, they are more related to performance requirements and the type of aircraft. Therefore, even if direct technological improvements exist, they may not be evident in the historical evaluation.

To model the evolution of technology that demonstrate a direct correlation with technological advancements, the Boltzmann Sigmoid, or S-curve, methodology was utilized. S-curves are characterized by four key parameters: the upper asymptote (U), indicative of the maximum achievable performance; the lower asymptote (La), representing the baseline performance; the inflection point (τ), where the rate of advancement transitions; and the growth rate (k), reflecting the pace of technological improvement. These parameters collectively delineate the progression from gradual improvements to rapid advancements and ultimately, the deceleration of gains as technologies reach maturity. To accurately determine the asymptotes of these S-curves, an investigation was conducted into the physical phenomena that could present barriers to technological advancement. These barriers include both inherent physical limitations and operational constraints, shaped by design requirements and regulatory standards. This approach ensures that the S-curves accurately reflect the theoretical and practical ceilings for technology advancement. Subsequently, historical data was fitted to these S-curves, with the quality of fit assessed using the coefficient of determination (R^2). During the fitting process, the lower and upper asymptotes were determined based on physical considerations which are discussed for each S-curve further in detail in Sec. III.C. The inflection point was selected based on the rapid improvement observed. Quasi-Newton optimization algorithms were applied to select the growth rate, enhancing the fit (the R^2 value) between the S-curve and the historical data on KPPs. The resulting S-curves and the considerations that went into each curve is discussed in detail in Sec. III.

The S-curve equation, as given in Eq. (3), utilizes the year of each data point (t) to model the progression of technological development. S-curves reflect the initial phase of gradual improvement, a rapid advancement toward the inflection point, and the final phase of slow performance improvements due to technology maturation. These phases can be seen in Fig. 1. Notably, technology development can undergo significant breakthroughs, necessitating the development of new S-curves for the metrics of interest.

$$S(t) = La + \frac{U - La}{1 + e^{-k*(t-\tau)}} \quad (3)$$

For non-technological projections, estimates were made based on the continuation of historical trends after understanding the physical drivers behind them.

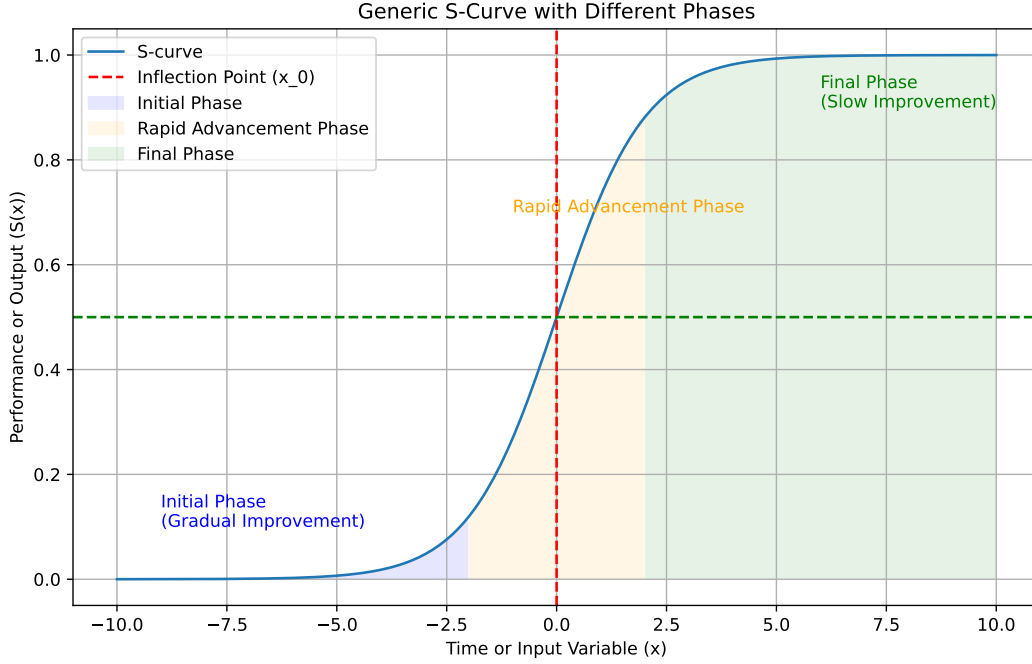


Fig. 1 Generic S-curve illustrating different phases of technological progression, including initial growth, rapid advancement, and maturation.

III. Examining Historical Trends and Future Projection

This section presents a historical evaluation of selected parameters (OEW/MTOW, T/W, TSFC, L/D) and future projections based on these trends. As described in Sec. II.B, data was collected from authorized sources, though certain aircraft were excluded from the analysis due to incomplete parameter information. Consequently, not all analyses include the same set of aircraft.

A. Operating-Empty-Weight-to-Maximum-Takeoff-Weight ratio (OEW/MTOW)

Aircraft design typically begins with weight estimations. For a given set of requirements, designers must estimate the payload weight ($W_{Payload}$), empty weight (W_{Empty}), fuel weight (W_{Fuel}), and maximum takeoff weight (MTOW, or W_0). One common approach in this process involves calculating weight fractions. Equation 4 illustrates the relationship among the operational empty weight fraction (W_{Empty}/W_0 , also denoted as OEW/MTOW), payload fraction ($W_{Payload}/W_0$), and fuel fraction (W_{Fuel}/W_0) [1].

$$\frac{W_{Empty}}{W_0} + \frac{W_{Payload}}{W_0} + \frac{W_{Fuel}}{W_0} = 1 \quad (4)$$

The fuel fraction mainly depends on mission requirements and performance characteristics, while payload weight is typically specified or inferred from design requirements. The operational empty weight relates to the aircraft

configuration and type, and is often regarded as an indicator of structural efficiency, reflecting how effectively an aircraft's structure is designed relative to its total weight capacity [5]. However, interpreting trends in OEW/MTOW requires careful consideration, as this ratio is influenced not only by technological advancements (e.g., improvements in material science or structural optimization) but also by market-driven factors such as design range, aircraft size, and payload capacity.

An example of this influence is shown in Fig. 2, which illustrates the relationship between aircraft range and OEW/MTOW. As range increases, OEW/MTOW tends to decrease because the aircraft must carry more fuel to cover longer distances. The observation that most aircraft with fewer than 125 passengers exhibit an OEW/MTOW ratio above 0.55 is consistent with the findings of Torenbeek, who reported a decreasing OEW/MTOW trend with increasing range [28]. However, Wolleswinkel and de Vries [29] indicate that achieving a ratio as low as 0.45 may be feasible.

Additionally, not all components contributing to OEW (such as landing gear, control systems, and electronic systems) scale proportionally with MTOW [30]. Consequently, larger aircraft generally have lower OEW/MTOW ratios, which is sometimes interpreted as a sign of higher structural efficiency. However, the trends discussed in the following paragraphs suggest that this decrease in OEW/MTOW cannot be directly attributed to improvements in structural efficiency alone.

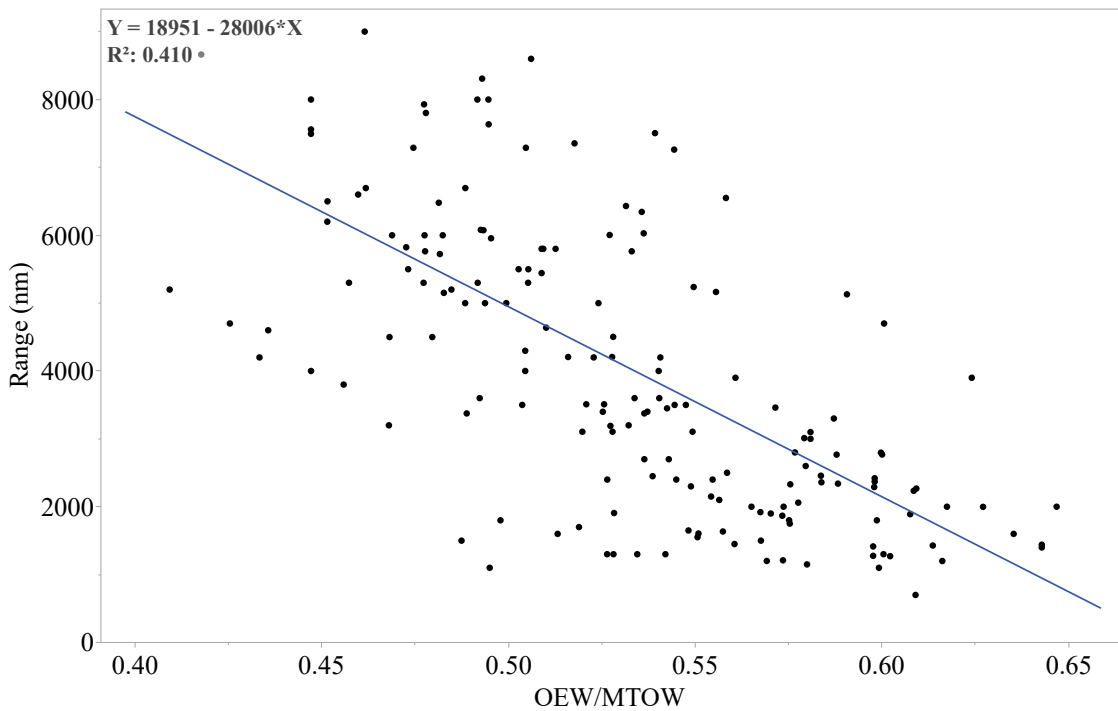


Fig. 2 Relationship between aircraft range and OEW/MTOW.

1. Study Design

The historical evolution of aircraft MTOW, size, range, and engine technology provides crucial insights into the drivers behind OEW/MTOW trends. To add more granularity, the aircraft in the database were categorized as either twin-aisle or single-aisle. The general trends shown in Fig. 3 suggest that OEW/MTOW has increased for single-aisle aircraft, with most data points concentrated between 0.5 and 0.6, while twin-aisle aircraft show a slight decrease over time.

The data was also color-coded based on range, classified as short (under 1500 nm), medium (1500–4000 nm), and long (over 4000 nm). Aircraft with missing range data are marked as ‘MS’ (green points). Figure 3 reveals that certain range groups deviate from the general OEW/MTOW trends. For instance, the trends for long-range twin-aisle aircraft appear to be insensitive to the aircraft certification date, suggesting the need for a more detailed analysis of the impact of range and other factors.

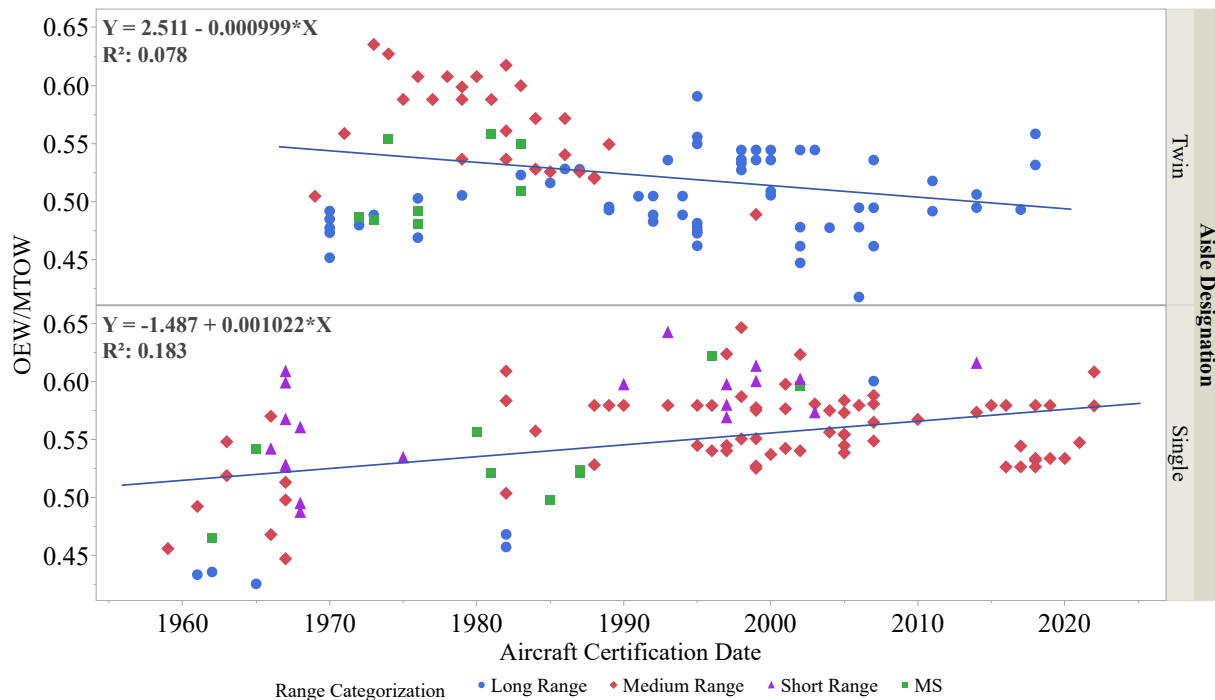


Fig. 3 Historical trends of OEW/MTOW for single-aisle and twin-aisle aircraft over time, color-coded by range classifications.

It should be noted that in Fig. 3, the OEW/MTOW ratios of some single-aisle aircraft produced between 1960 and 1970 were generally below the overall trend. These aircraft typically had four engines and were designed for medium- to long-range capabilities. Due to the lower efficiency of engines during that period, these aircraft carried more fuel (as later shown in Fig. 9), resulting in lower OEW/MTOW ratios. For twin-aisle aircraft, models produced between 1970

and 1990 were often medium-range, leading to higher OEW/MTOW values. Later, medium-range aircraft began to be produced as single-aisle models.

2. Impact of Range, Size, and MTOW

Figure 4 shows that the range of twin-aisle aircraft has gradually increased, reflecting design choices favoring long-haul capability. However, there is no clear trend of range growth for single-aisle aircraft, as indicated by the low R^2 value. This suggests that designs in this category prioritize cost-efficiency and short-haul performance rather than extending range.

Similarly, Fig. 5 indicates an increase in the size of twin-aisle aircraft over time, with Fig. 6 showing a corresponding rise in MTOW. In contrast, the size and MTOW of single-aisle aircraft do not exhibit consistent growth, reflecting their role in short- to medium-range operations where flexibility and economic considerations are prioritized over size increases.

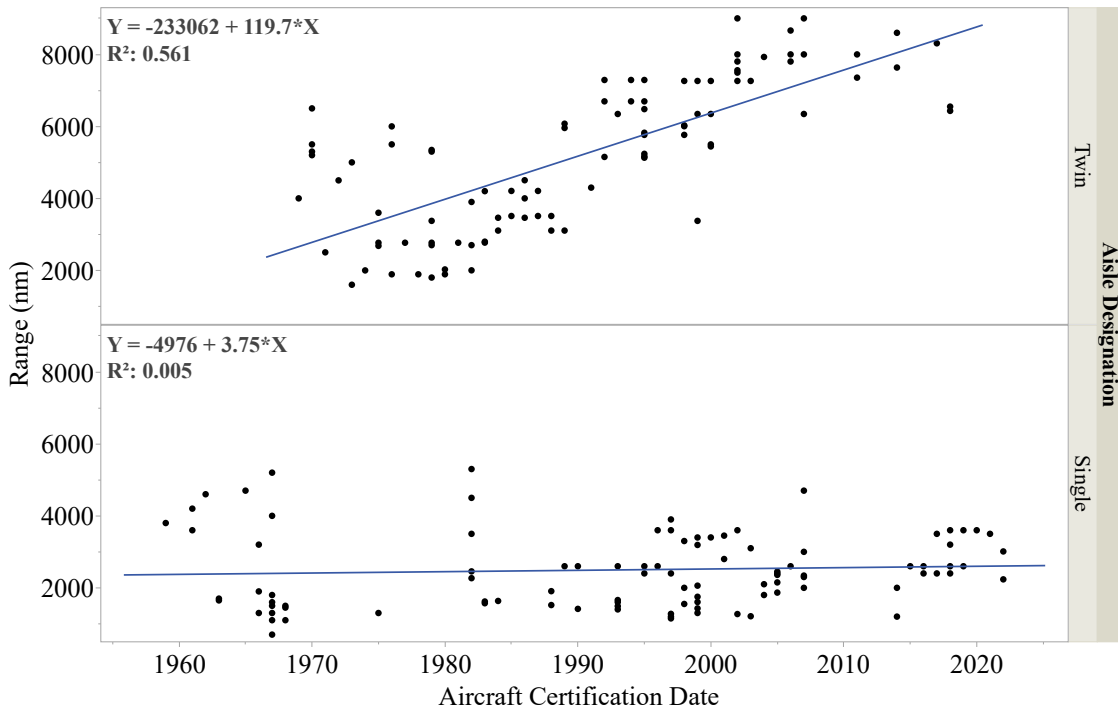


Fig. 4 Evolution of aircraft range over the years for single-aisle and twin-aisle configurations, demonstrating differences in range trends.

3. Influence of Engine Weight

Figure 7 reveals that the engine weight fraction for twin-aisle aircraft has decreased over the years, while it has slightly increased for single-aisle aircraft, despite no consistent rise in MTOW (as seen in Fig. 6). Engine weight is part of the operating empty weight, and these trends align with the OEW/MTOW patterns observed in Fig. 3. This suggests

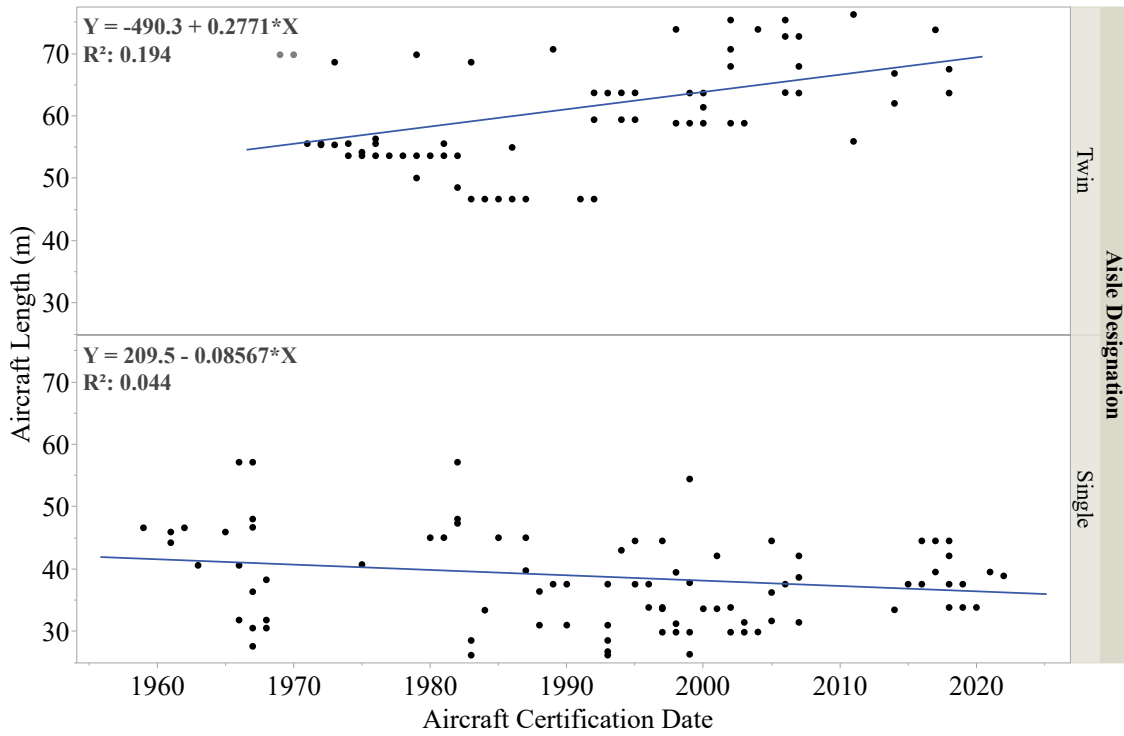


Fig. 5 Change in aircraft length over time for single-aisle and twin-aisle aircraft.

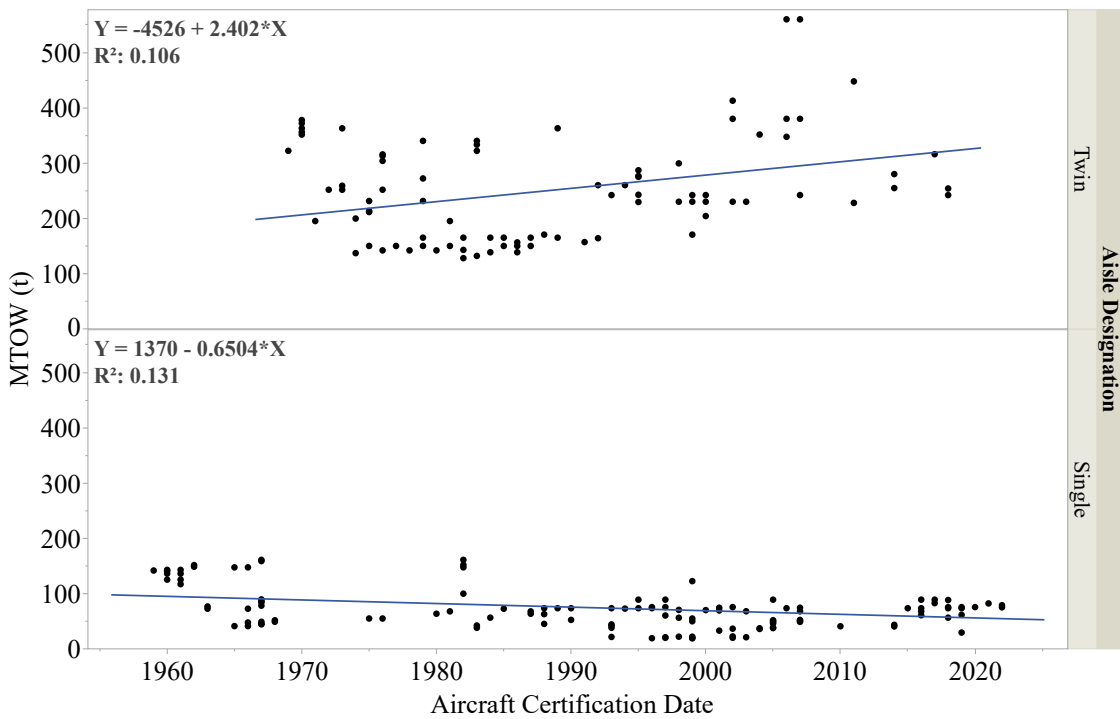


Fig. 6 Maximum takeoff weight trends for single-aisle and twin-aisle aircraft over the years.

that changes in engine weight fraction also likely contribute to the overall OEW/MTOW trends. Thus, the rising trend in OEW/MTOW for single-aisle aircraft is potentially impacted by the higher engine weight fraction. While the weight of the integrated propulsion system may trend better with weight, engine manufacturers and certification sheets report the dry weight of their engines. Nacelle, pylon, and other installation weights are beyond the resolution of reported weight breakdowns.

4. Other Factors

Trends in aircraft design reflect competing pressures on OEW/MTOW. Improvements in passenger comfort, including the incorporation of heavier seating and onboard entertainment systems, along with advancements in safety and reliability technologies, have likely contributed to increases in OEW/MTOW over time [5, 28]. However, recent initiatives have sought to mitigate these increases through cabin redesigns and lightweight seating. Although seat masses are difficult to isolate quantitatively, several sources provide approximate estimates.

The Aerospace Technology Institute's FlyZero project estimated a total seat mass of approximately 1,600 kg for a low-cost carrier (LCC, all economy class) configuration of an Airbus A320 [31]. Assuming 180 seats, this corresponds to an average seat mass of 8.9 kg. This value is consistent with figures cited by Dubois, who reported a range of 8–15 kg per seat [32]. Applying the 8–15 kg range to a 180-seat layout yields a total seat mass between 1,440 kg and 2,700 kg. Relative to a typical A320neo OEW of approximately 42,600 kg, seat mass would constitute 3.4–6.3% of OEW. LCC configurations can underestimate seat weight however, since business class seating can weigh up to 80 kg per seat [32]. A study by Fuchte et al. [33] found that cabin redesigns can reduce OEW by up to 12%, resulting in fuel savings of up to 9%. Given that lighter seats can provide fuel burn benefits and be easily retrofitted into existing aircraft, there is market demand for a next generation seat. Expliseat, a light-weight seat manufacturer, has certified lightweight seats for ATR aircraft, Embraer E-Jets, and the Airbus A320 family [34]. The company claims reductions of up to 30% in seat mass compared to conventional designs, although higher procurement costs remain a barrier to widespread adoption [32].

Another influence on OEW/MTOW, outside of mission and market demands, may be environmental regulations regarding noise (and to a lesser extent emissions), which play a role in dictating takeoff-field performance, especially for single-aisle aircraft operating at noise-sensitive, landlocked airports. Aircraft must meet ICAO Chapter 4 (and, increasingly, Chapter 14) noise limits under FAR Part 36 [35]. Achieving compliance often requires heavier acoustic treatments such as liners inside engine nacelles and pylons, chevroned nozzles or other hush-kit hardware, more complex high-lift systems due to treated surfaces, and landing gear fairings [36]. These noise insulating structures add directly to OEW. Moreover, many urban or landlocked airports mandate Noise Abatement Departure Procedures (NADP) [37], which impose steep climb gradient requirements. To meet these requirements while using reduced-thrust takeoff settings (to minimize noise near the runway), engines must still be capable of achieving steep climb gradients. This may require airlines to select slightly up-rated (i.e., heavier) engines, further increasing OEW.

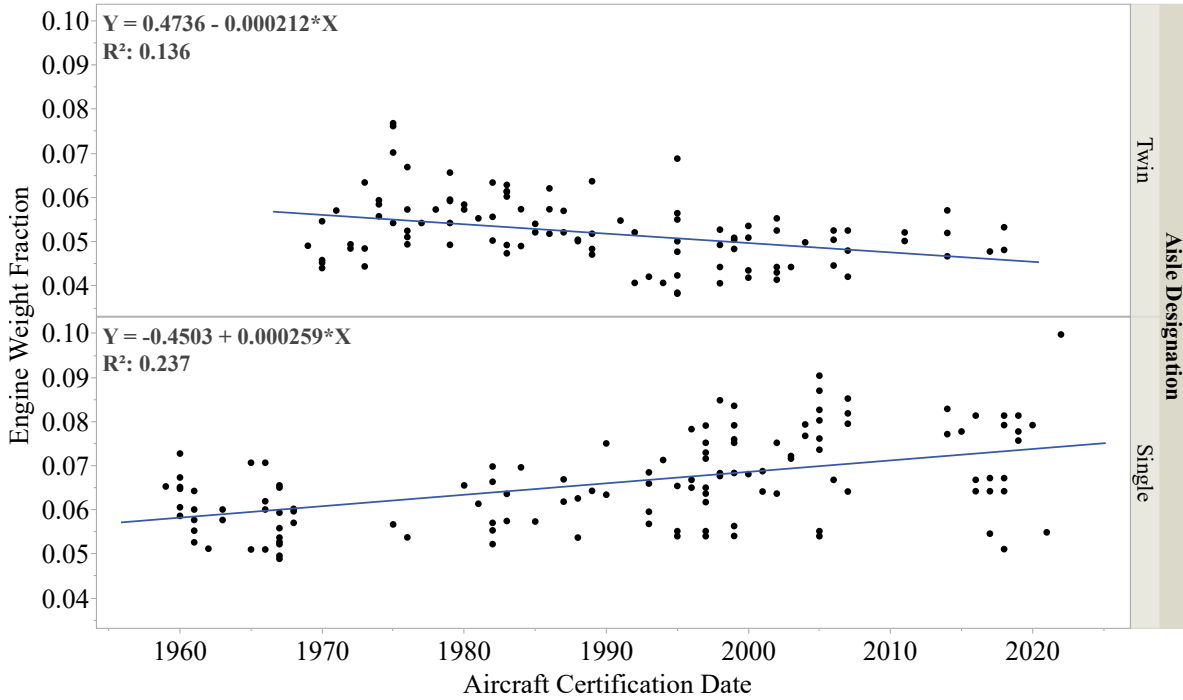


Fig. 7 Trends in engine weight fraction over time, grouped by single-aisle and twin-aisle aircraft.

5. Material Technology and Structural Efficiency: A Case Study

The analyses thus far show that it is rather challenging to directly attribute changes in this ratio to material advancements, such as composites and lightweight aluminum, solely based on the historical trends of OEW/MTOW. Even where these materials have been adopted, their effects may not be immediately evident from broad historical analyses. However, this does not imply that material improvements have no influence on empty weight fraction. To accurately assess the impact of lightweight materials on OEW/MTOW, a direct comparison of aircraft with similar top-level design requirements, such as passenger capacity and range, would be necessary.

To explore this hypothesis, two aircraft with similar design requirements are compared in Tab. 1. The top-level design parameters of the A330-900, certified in 2018, and the A350-900, certified in 2014, are fairly similar. For instance, the A330-900 has a passenger capacity of 310 and a range of up to 7,200 nm, while the A350-900 can carry 315 passengers and fly up to 8,300 nm. Their overall dimensions are also similar. The A350-900 is primarily constructed using composite materials, whereas the A330-900 is mostly made of aluminum [38]. Comparing the OEW/MTOW ratios, the A350-900 has a 10% lower operational empty weight fraction. Given the similarity in design and performance parameters between these two aircraft, in addition to the other factors mentioned above (such as amenities), the lower OEW/MTOW of the A350-900 may be attributed to the use of composite materials.

Table 1 Comparison of A330-900 and A350-900 [10].

Aircraft	Length, m	Wingspan, m	Range, nm	Passengers (2-Class)	OEW/MTOW
A330-900	63.66	64.00	7,200	310	0.559
A350-900	66.80	64.75	8,300	315	0.506

6. Fuel Fraction Trends and Cost Efficiency

When examining the changes in fuel fraction over the years (Fig. 9), it is clear that the fuel fraction for twin-aisle aircraft has not increased at the same rate as their range (Fig. 4), implying improvements in fuel efficiency. However, the low R^2 value for twin-aisle aircraft fuel fraction trends indicates a weak correlation, implying that while the general trend points to efficiency gains, there are other factors (such as engine or aerodynamic improvements) influencing fuel consumption. Conversely, the range trends for single-aisle aircraft have remained relatively stable (Fig. 4), as has their payload capacity (Fig. 8), yet a significant reduction in fuel fraction is observed. This pattern, coupled with a weak correlation in R^2 for range and fuel, indicates that other factors have led to fuel savings even without extending range capabilities. These improvements align with broader trends towards operational efficiency in the single-aisle segment, where maintaining low operational costs per passenger per unit of range is a key objective.

Figure 10 illustrates changes in this cost metric over the years for both twin-aisle and single-aisle aircraft, showing a consistent decline. The stronger R^2 values suggest that these reductions have been a significant and reliable trend, driven by advances in propulsion, aerodynamic refinements, and weight optimization. While fuel efficiency has been a major factor in reducing costs, improvements in structural efficiency (as seen in OEW/MTOW) are less evident in broad historical evaluations.

7. Summary and Future Evaluation of OEW/MTOW Trends

In summary, trends in the OEW/MTOW ratio do not directly reflect structural efficiency. Evaluations of aircraft structural efficiency must take into account high-level design requirements, such as range and aircraft size. Although historical data for conventional aircraft demonstrate variations in OEW/MTOW ratios over time, no radical changes have been observed thus far. For future projections of conventional aircraft, assuming relatively stable market demand and constant factors such as aircraft size, MTOW, and range, the average OEW/MTOW ratio—calculated as the mean of historical data—is approximately 0.56 for single-aisle aircraft and 0.51 for twin-aisle aircraft in Figure 3. However, recent discussions and studies in aviation have increasingly focused on unconventional aircraft configurations such as blended wing body (BWB) and alternative propulsion systems, including hybrid-electric and hydrogen-powered aircraft. Qian and Alonso [39] performed structural optimization on the BWB configuration to estimate its structural weight. They obtained an OEW/MTOW ratio of 0.47, which is similar to that of conventional aircraft designed for the same mission profile. Scholz concluded in his study [40] that BWB configuration does not significantly improve the

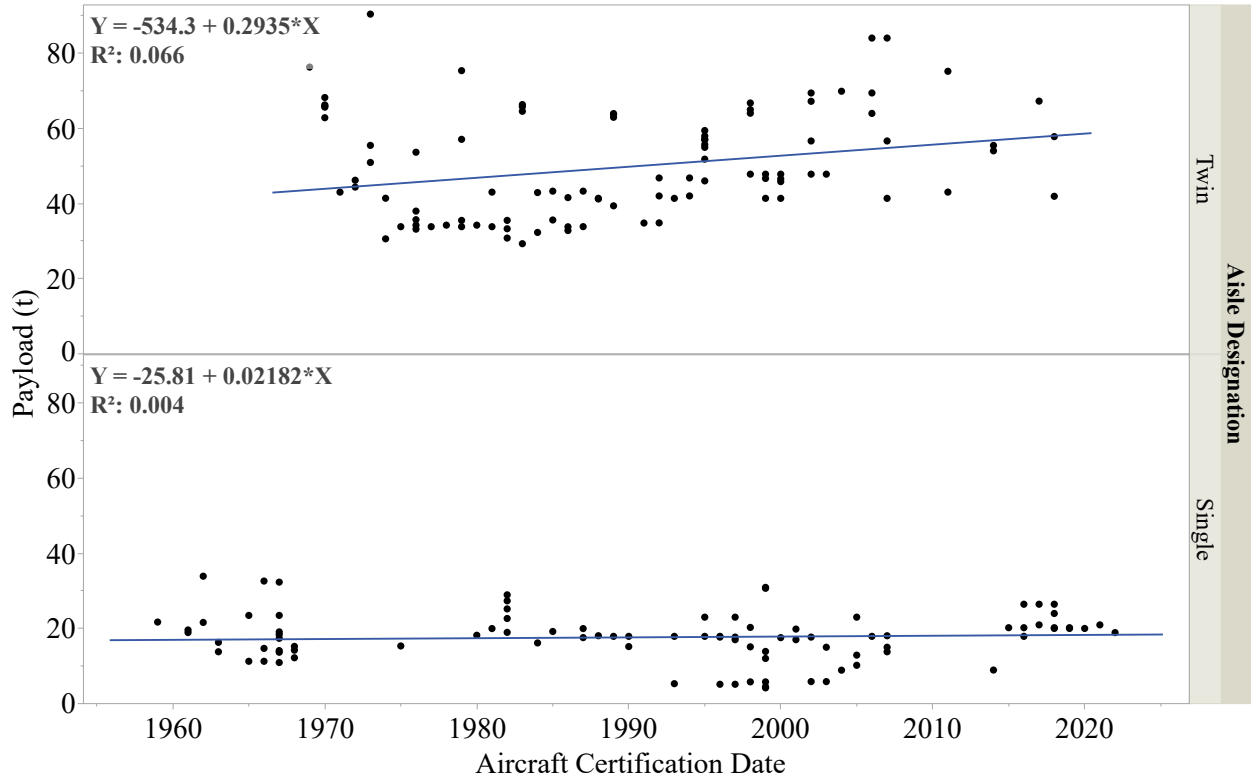


Fig. 8 Historical payload capacity trends for single-aisle and twin-aisle aircraft.

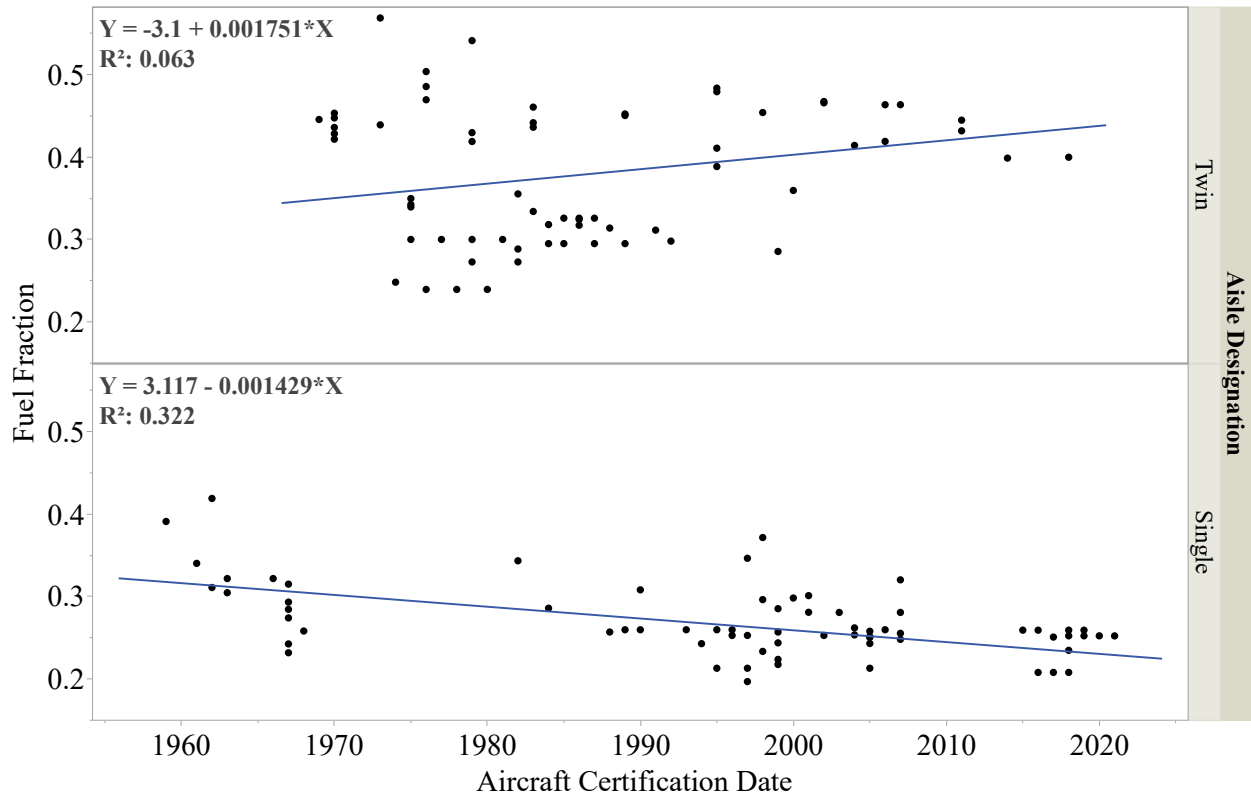


Fig. 9 Evolution of fuel fraction over time for single-aisle and twin-aisle aircraft.

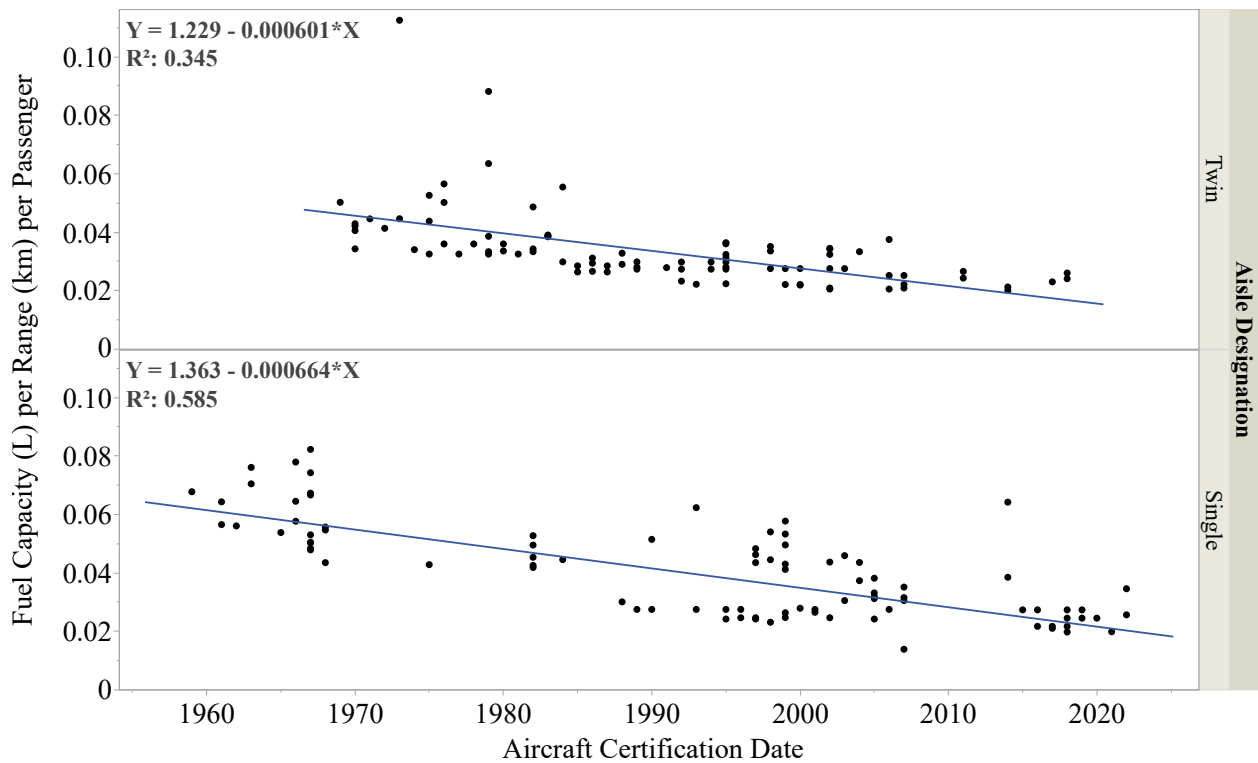


Fig. 10 Trends in fuel efficiency measured as fuel capacity per range per passenger for single-aisle and twin-aisle aircraft, showing the reduction over time.

OEW/MTOW ratio compared to conventional designs.

Hydrogen propulsion and hybrid-electric aircraft introduce significant design changes, particularly in weight distribution and propulsion system architecture. Consequently, OEW/MTOW for these configurations can differ markedly from that of conventional aircraft. For instance, Xisto and Lundbladh [41] report that liquid hydrogen-powered aircraft have an OEW/MTOW ratio of 0.688, a 43% increase over the 0.48 ratio observed in comparable tube and wing designs. Electrified aircraft concepts, whether partially or fully battery-powered, also tend to exhibit higher OEW values, primarily due to the substantial mass of batteries imposed by current technology limitations [42, 43]. Such aircraft are unlikely to follow the conventional development trajectory. Instead, their progress is closely linked to advancements in gravimetric energy density, power density and related technologies.

These observations imply that aircraft employing alternative propulsion systems follow distinct development paths, characterized by unique OEW/MTOW trends. Rather than adhering to conventional evolutionary trajectories, such configurations will likely exhibit their own S-curves in terms of technological maturity and performance improvements [44].

B. Thrust-to-Weight ratio (T/W)

The thrust-to-weight ratio (T/W), defined as the ratio of sea-level static thrust to maximum takeoff weight of the aircraft, is a crucial parameter influencing aircraft performance and is closely related to the wing loading (W/S), the ratio of MTOW to the aircraft's wing area [1, 45].

Analyzing the relationship between the four main forces acting on an aircraft, namely thrust, drag, lift, and weight, yields a functional connection between T/W and W/S. Mattingly represents this relationship in Eq. 5, referred to as the “constraint master equation” [45]. This equation establishes constraint boundaries for T/W and W/S, derived from both aircraft design requirement and regulatory constraints, such as cruise speed, turn rate, climb rate, approach speed and takeoff field length. Figure 11 illustrates a sample constraint diagram, with W/S on the horizontal axis and T/W on the vertical axis. Once all constraints are defined, the objective is to minimize the T/W ratio and select the optimal point in the solution space. Both T/W and W/S are typically selected early in the design phase [45].

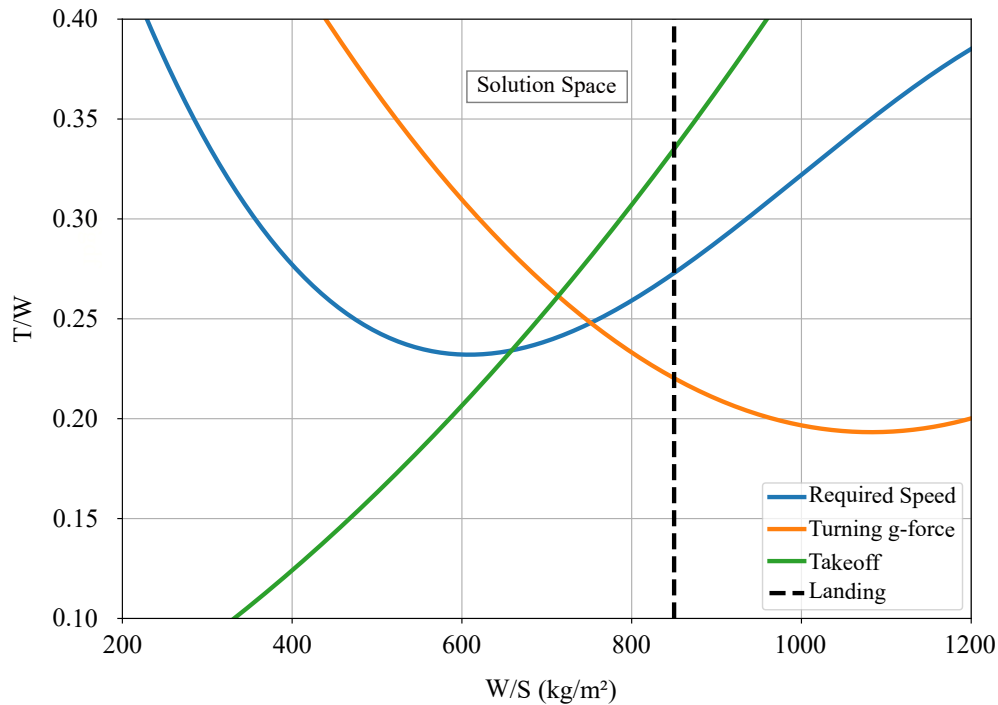


Fig. 11 Notional constraint diagram illustrating thrust-to-weight (T/W) ratio versus wing loading (W/S), based on performance constraints. Weight in this instance refers to MTOW.

When investigating T/W over the years in Fig. 12, values range from 0.21 (corresponding to the DC-8-31) and 0.42 (corresponding to the CRJ 550). T/W ratio increases roughly 1.1% per decade, however is not expected to continue unbounded. Increases in T/W ratio achieved through larger engines incur weight penalties, while those achieved through airframe weight reduction can incur significant cost penalties due to the reliance on advanced lightweight materials. To understand the reasons behind these trends, aircraft were categorized by aisle configuration, as shown in Fig. 13.

Observing the thrust-to-weight (T/W) ratio trends for both twin-aisle and single-aisle aircraft, it can be seen that the T/W ratio is increasing for single-aisle aircraft, while no clear trend is seen for twin-aisle aircraft. Primary influences of these trends are explored in the following subsections.

1. Influence of Maximum Engine Thrust and MTOW

Figure 14 shows the maximum takeoff thrust of engines from 1956 to 2020, categorized by aisle designation. Maximum thrust ratings for engines used in twin-aisle aircraft have significantly increased over time, whereas only a slight increase is observed in the single-aisle category. In single-aisle aircraft, the increase in the T/W ratio, along with improved fuel efficiency, stems from a reduction in MTOW and an increase in thrust. For twin-aisle aircraft, although engines with higher thrust were developed, the weight of the aircraft on which these engines are installed has also increased proportionally with thrust, resulting in no clear trend in T/W change. In the database, the most powerful engine is recorded as the GE9-115B, producing 513.9 kN of thrust, while the least powerful is the ALF502R-3A, producing 31 kN—over 16 times less thrust than the GE9-115B. However, this variation in thrust levels does not directly indicate changes in the T/W ratio, as T/W is highly influenced by design requirements, regulatory constraints, and weight, as discussed previously. Additionally, T/W is closely related to W/S, and not dependent solely on the engine technology.

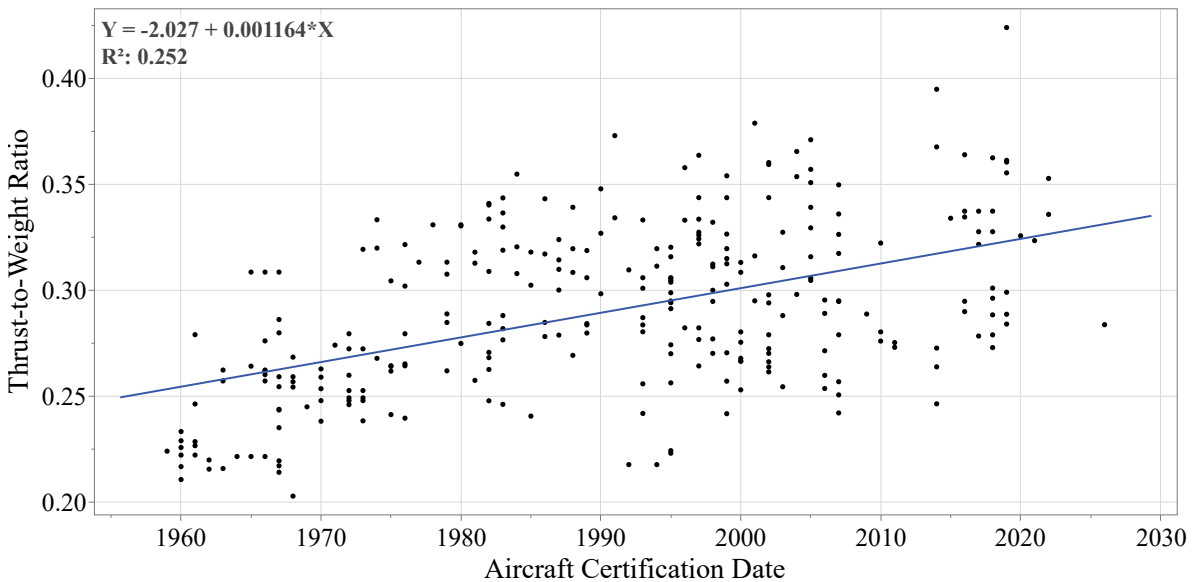


Fig. 12 Historical trends in thrust-to-weight ratio for aircraft.

2. Influence of Aircraft Type, Mission, and Performance Requirements

In the early design phase, Raymer [1] categorizes T/W based on intended aircraft use, such as military, fighter, or transport applications. The categorization further divides fighter aircraft into subcategories like trainers and dogfighters,

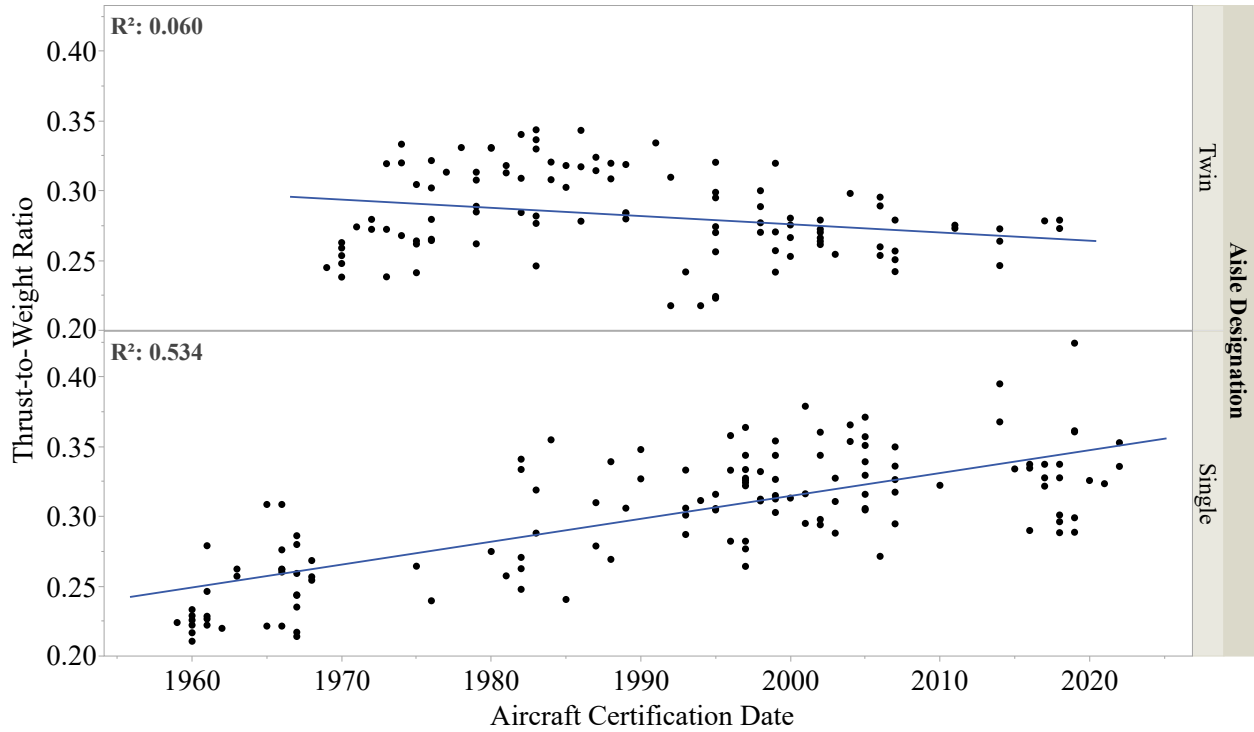


Fig. 13 Historical trends in thrust-to-weight ratio for aircraft by aircraft aisle designation.

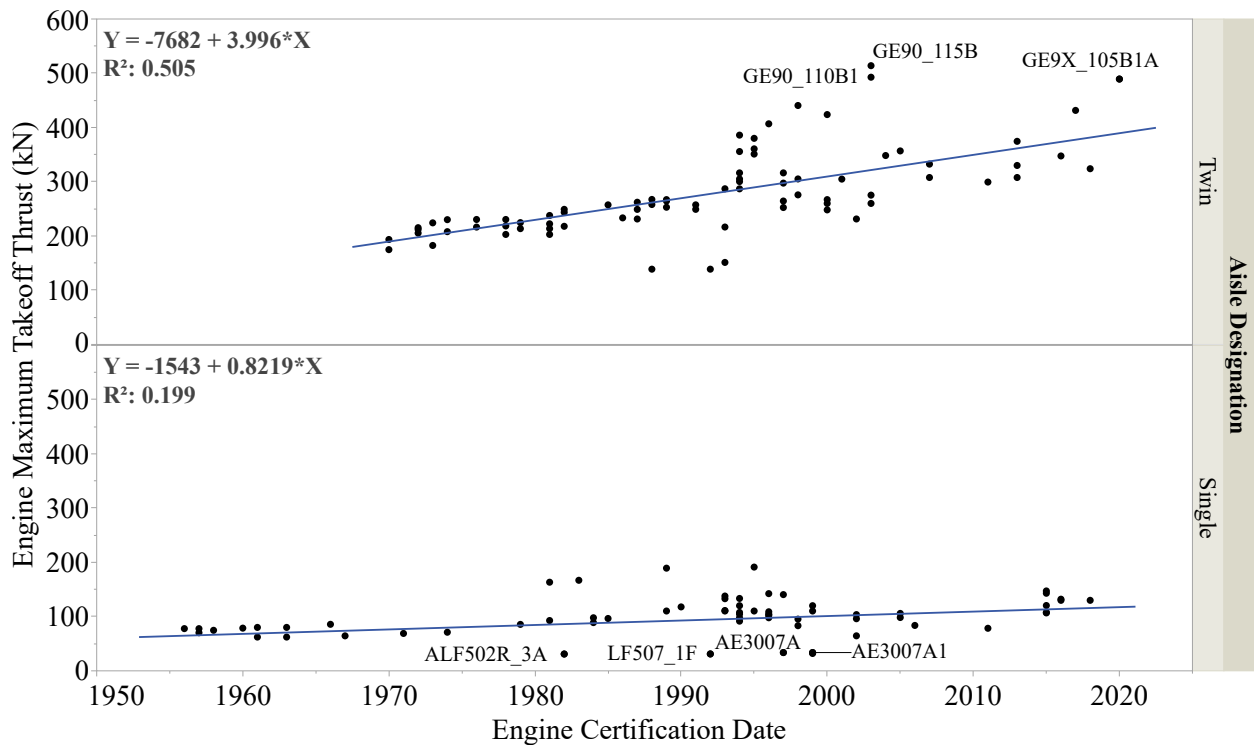


Fig. 14 Maximum takeoff thrust of engines over time, color-coded by aircraft aisle designation, illustrating the evolution of engine performance.

emphasizing that T/W directly reflects mission-specific performance parameters.

An example on the impact of performance requirements on T/W is the takeoff field length and its effect on T/W requirements, as shown in Fig. 15. Aircraft with lower T/W ratios require longer takeoff distances because T/W directly affects acceleration, meaning a longer runway is needed to reach takeoff speed—impacting airport compatibility and operational requirements. Alternatively, this trend can also be viewed from the perspective that aircraft designed to operate from longer runways can opt for less powerful engines, potentially reducing costs and saving weight. Both interpretations imply that knowing the required takeoff field length early in the design process enables optimization of T/W for specific field length constraints.

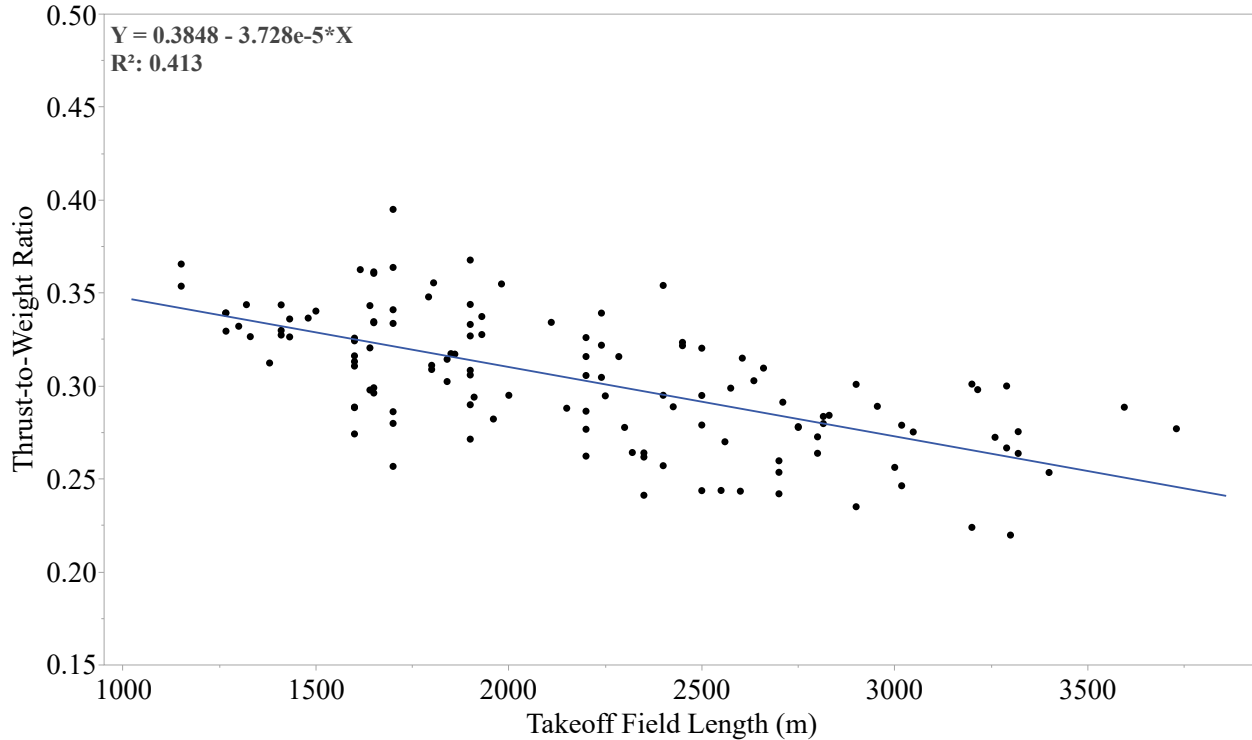


Fig. 15 Relationship between thrust-to-weight ratio and takeoff field length, demonstrating performance trade-offs.

3. Other Factors

Equation 5 defines the parameter β as the ratio of the instantaneous weight W to the takeoff weight W_{TO} , represented as $\beta = \frac{W}{W_{TO}}$ [45]. This parameter depends on fuel efficiency and payload delivery. Fuel efficiency increases over time, as seen in Fig. 10, which may play a role in the increase of the T/W ratio. The impact of noise abating regulations, discussed in detail in Sec. III.A.4, may also play a role in the apparent increasing trends in T/W for single aisle aircraft.

$$\frac{T}{W} = \frac{\beta}{\alpha} \left(\frac{qS}{\beta W} \left[K_1 \left(\frac{n\beta W}{qS} \right)^2 + K_2 \left(\frac{n\beta W}{qS} \right) + C_{D0} + C_{DR} \right] + \frac{P_s}{V} \right) \quad (5)$$

Increases in engine bypass ratio over time may also be responsible for the apparent increase in T/W. Engine data shown is as the engine manufacturers report it, therefore down-rated (or up-rated) thrusts are not included. If higher bypass ratio engines require scaling, the larger engine may be overpowered for its application at the benefit of better fuel economy. Figure 16 illustrates the relationship between bypass ratio and thrust to weight ratio. The generational categories are immediately apparent, and representative engines from each era are labeled for readability. While there is a large spread of T/W values at each bypass ratio group, single aisle aircraft seem to exhibit a generally increasing T/W with increasing bypass ratio, supporting the hypothesis that higher bypass ratios in recent years have increased T/W ratios above what may be required by a mission.

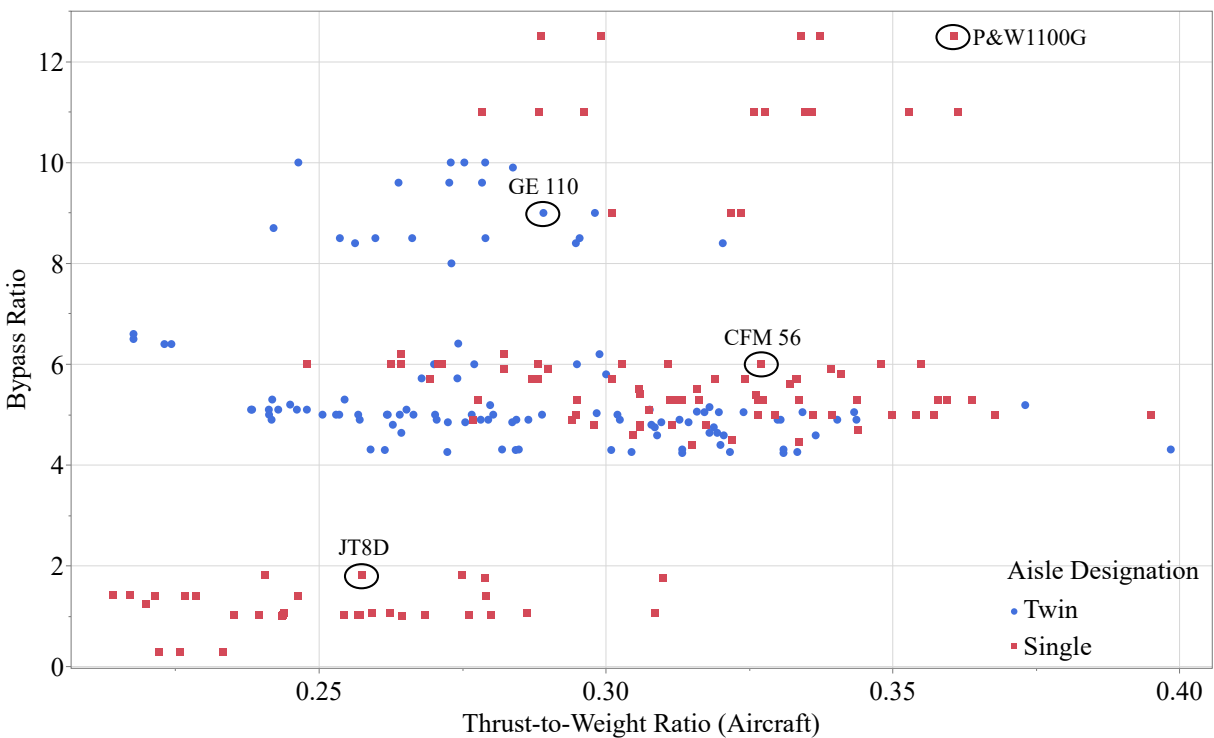


Fig. 16 Bypass Ratio vs Aircraft T/W, differentiated by aisle designation. Well-known engine labels included to show generational differences.

4. Summary and Future Evaluation of T/W Trends

T/W ratio depends on the aircraft type, fuel efficiency, and performance requirements. In this paper, only conventional subsonic transport aircraft are considered, and the T/W ratios observed range between 0.21 and 0.42, varying according to the aircraft's specific performance parameters. It is anticipated that future performance requirements for conventional aircraft configurations—such as cruise speed, service ceiling, and turning rate—will not undergo significant changes. Additionally, engine thrust is not expected to increase as significantly as in previous years. Thrust positively correlates

with the bypass ratio; thus, higher bypass ratios result in greater thrust and larger engine diameters, as illustrated in Fig. 18. However, ongoing improvements in bypass ratio will eventually encounter limitations due to ground clearance constraints [46].

Increases in bypass ratio improve propulsive efficiency by moving a larger volume of air and exhausting it at velocities closer to that of the freestream (as opposed to that of the core). Thrust production is proportional (equal if the exhaust is ideally expanded) to $\dot{m}(V_e - V_\infty)$, and as seen in Eq. 6, propulsive efficiency is maximized when the exhaust velocity is equal to the freestream velocity. This implies that in order to maximize engine efficiency while producing the same amount of thrust, the difference between exhaust and freestream velocities should be reduced while moving as large of a volume of air as possible, consistent with trends in increasing bypass ratio.

However, propulsive efficiency alone does not define the efficiency of the propulsion system. Thermal efficiency is as important as propulsive. As seen in Eq. 7, the thermal efficiency of a heat engine is maximized when the difference between the heats of the fluid before and after addition of energy is maximized. Real gas effects, material temperature limits, and environmental concerns limit the temperature at which air in the engine can be raised to in practice, although improvements in thermal efficiency are an active area of research, and are discussed in the following section.

$$\eta_p = \frac{2}{1 + \frac{V_e}{V_\infty}} \quad (6)$$

$$\eta_{\text{therm}} = 1 - \frac{Q_0}{Q_f} \quad (7)$$

Propulsive efficiency is improved through changes in engine design, however the absence of strong correlations between time and engine thrust, as shown in Fig. 14, suggests that engine efficiency gains are realized at marginally different thrust levels. Figure 16 quantifies the correlation between bypass ratio and T/W, which does not show a clear trend. While changes in engine design may have an effect on the thrust an engine produces, the choice of engine and T/W ratio is likely driven primarily by an aircraft's mission requirements.

Thermal efficiency improvements, effected through higher combustion temperatures, do not necessarily correlate with T/W either. Figure 17 shows that T/W does not show a clear trend with turbine exit (core exhaust) temperature. While exit temperature is affected by temperature drops in the turbine, Fig. 17 also shows that turbine entry temperature and turbine exit temperature are weakly correlated. If the outlier, the CF6-80CA5, is removed, the R^2 value improves to 0.901, which can be called a strong correlation. This illustrates how, similar to bypass ratio and propulsive efficiency, combustion temperatures and thermal efficiency are not primary drivers of T/W.

However, unconventional configurations, such as the BWB, fundamentally differ from conventional aircraft in terms of wing loading and aerodynamic efficiency, significantly affecting the T/W ratio. Studies predict that BWB aircraft will likely exhibit a lower T/W ratio compared to conventional configurations [47]. Additionally, hydrogen-powered aircraft

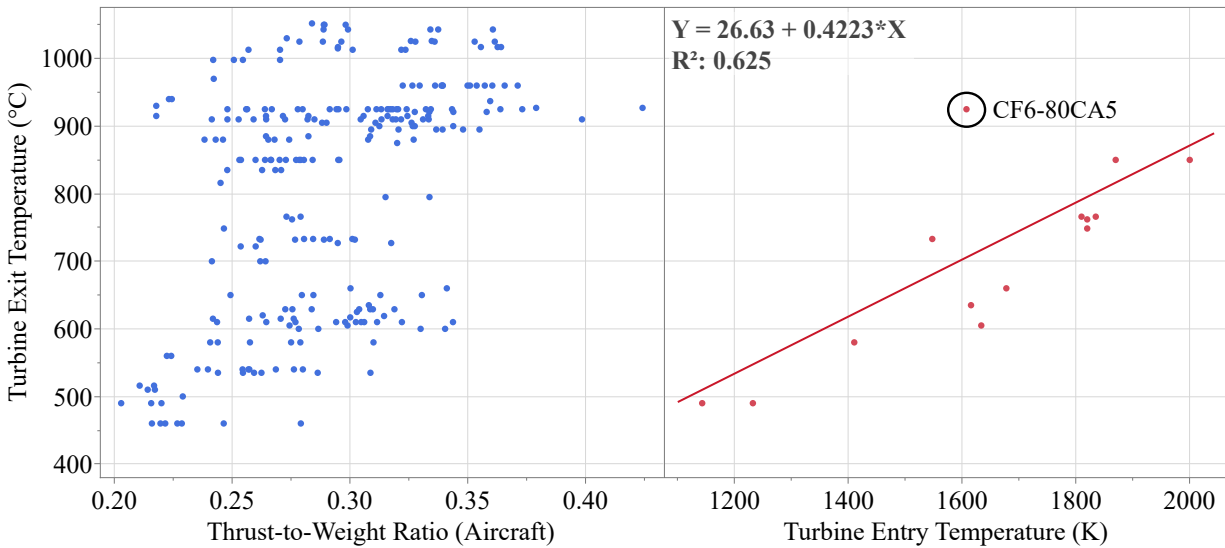


Fig. 17 Turbine exit temperature vs aircraft thrust-to-weight ratio and turbine entry temperature. The outlier, the CF6-80CA5, is called out. If ignored, the coefficient of determination improves from 0.625 to 0.901 for a linear map between turbine entry and exit temperatures.

are anticipated to exhibit higher T/W ratios due to their larger liquid hydrogen storage tanks and modified fuselage designs, which result in increased wetted surface areas. One study by Xisto and Lundbladh [41] compared a Jet-A and liquid hydrogen powered aircraft. Both of these aircraft assumed some notional increases in technology levels by the year 2050, as well as both being installed into a tube and wing architecture. The liquid hydrogen aircraft required a T/W 16% higher than its Jet-A counterpart, despite its 3% lower MTOW. The study attributes this to an increase in wing and wetted surface areas. Furthermore, changes in performance parameters and operational requirements, such as cruise speed and takeoff field length, may also contribute to variations in the T/W ratio.

In summary, although conventional aircraft are unlikely to significantly deviate from historical trends in T/W ratios, unconventional aircraft configurations could experience substantial changes compared to existing standards, as they follow their own distinct evolutionary paths.

C. Thrust Specific Fuel Consumption (TSFC)

In aircraft design, fuel efficiency is a critical performance metric, with Thrust Specific Fuel Consumption (TSFC) serving as a measure of the fuel efficiency for turbofan engines [45]. TSFC is defined as the fuel consumption per unit time normalized by thrust [48]. Lower cruise TSFC values reflect more efficient propulsion systems, and advancements in propulsion technology have led to notable TSFC reductions over time, as seen in Fig. 19. The cubic fits shown in Fig. 19 may (or may not) trend well with the data, however it is important to note that the fits are purely statistical, and cannot be used to project trends into the future.

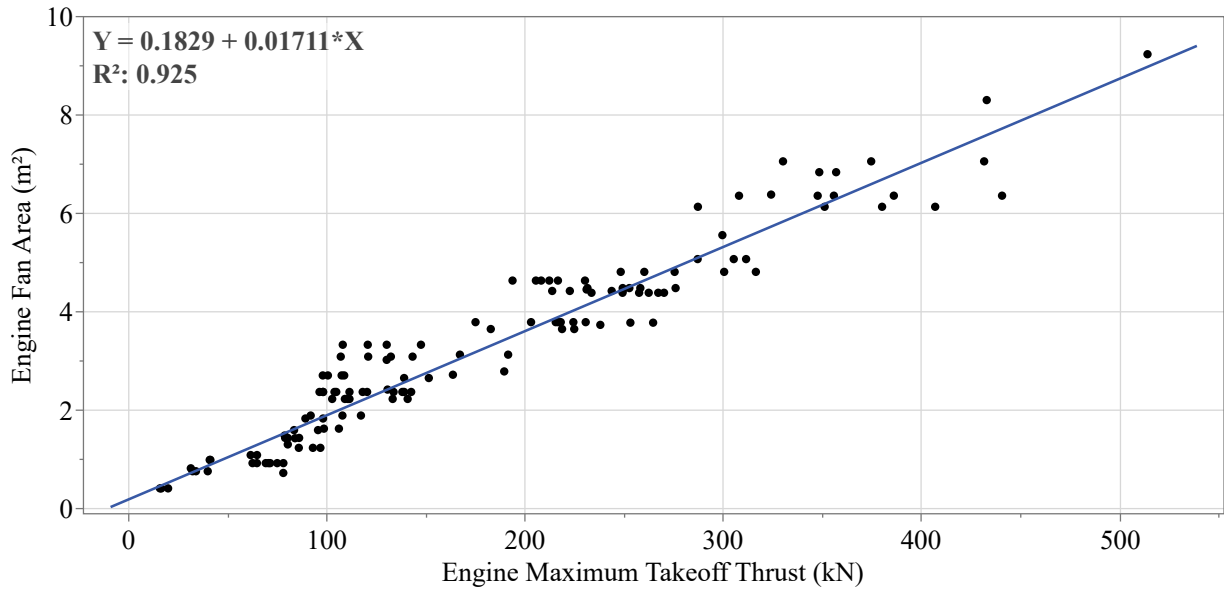


Fig. 18 Correlation between engine diameter and maximum takeoff thrust, highlighting engine design trends over time.

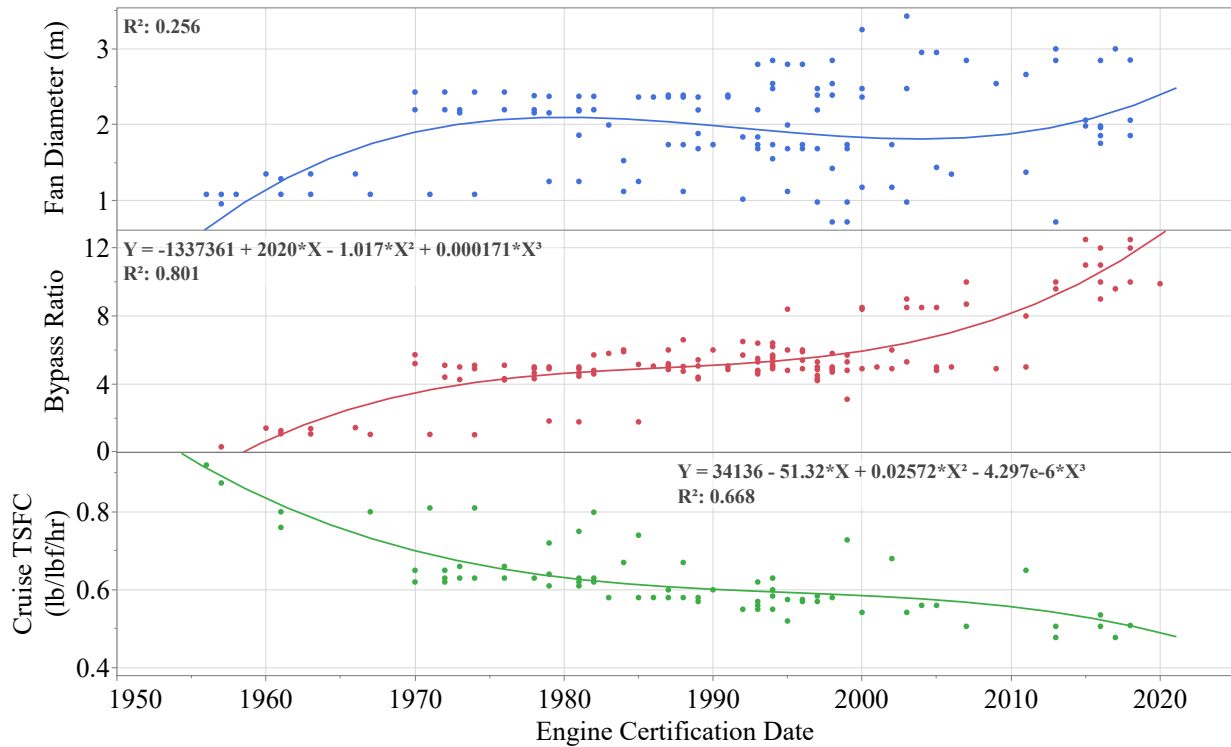


Fig. 19 Trends in fan diameter, bypass ratio, and thrust-specific fuel consumption relative to the engine certification year.

1. Factors Influencing TSFC Trends

While TSFC trends show a general decline with newer engine designs, several performance factors influence gas turbine efficiency. Studies from the National Academies of Sciences, Engineering, and Medicine (NASEM) in 2016 identified key engineering drivers in engine design: overall efficiency, weight, drag, and reliability [49]. Overall efficiency encompasses the efficiency with which the engine converts the chemical energy stored in fuel to propulsive power. Current trends indicate that increases in propulsive efficiency demand larger engines, costing additional weight and drag. As such, committees in NASEM note that engines for long-range or twin-aisle applications are optimized for higher efficiency levels due to the weight and cost studies for engine weight and fuel burn. Smaller or single-aisle aircraft favor smaller engines with cheaper cost of ownership and are not as efficient as ones used on twin-aisle aircraft.

Figure 20 illustrates that TSFC decreases as both engine diameter and bypass ratio increase, while Fig. 19 shows bypass ratio increase over time. These trends reflect efficiency gains from engine designs with high bypass ratios. Interestingly, the fan diameters of the engines increase much less dramatically as time passes, suggesting that increases in bypass ratios are primarily achieved through core miniaturization. This is corroborated by the previously discussed relationship between bypass ratio and T/W, illustrated in Fig. 16. Achieving larger bypass ratios through increasing the absolute size of engines at similar power outputs is ultimately undesirable as the additional fan drag requires a larger T/W, and consequently a larger OEW/MTOW, both of which oppose this avenue towards TSFC improvements through increasing bypass ratio without downsizing the engine core. Figure 21 directly compares bypass ratio and fan diameter, which shows slight positive correlation. This indicates a potential secondary influence of engine scaling on bypass ratio. Since the area of a circle or annulus scales with its radius squared, the ratio of bypass area to core area (bypass ratio) grows nonlinearly as engines increase in absolute size.

Torenbeek's high-level TSFC expression in Eq. (8) [28] accounts for factors such as cruise Mach number M_o , cruise ambient to sea level temperature ratio θ , and overall engine efficiency η_{tot} , which combines propulsive and thermal efficiencies. This equation highlights the physical determinants of TSFC, including maximum cruise altitude, air temperatures at cruise and sea level, and engine component efficiencies.

$$SFC = 0.2788 * \frac{M_o * \sqrt{\theta}}{\eta_{tot}} \quad (8)$$

The present scope of the study encompasses only conventional subsonic transport aircraft, which limits the consideration of cruise Mach number to less than unity. Based on the historical maximum operating cruise Mach number data shown in Fig. 22, turbofans typically cruise between Mach 0.7 and 0.95.

It was noted in data collection that TCDSs often record only the maximum operating cruise Mach number instead of the typical cruise Mach number, as the latter can vary depending on the flight mission profile. However, a limited number of aircraft manufacturer's Airport Planning Manuals (APM) payload-range diagrams, which document actual

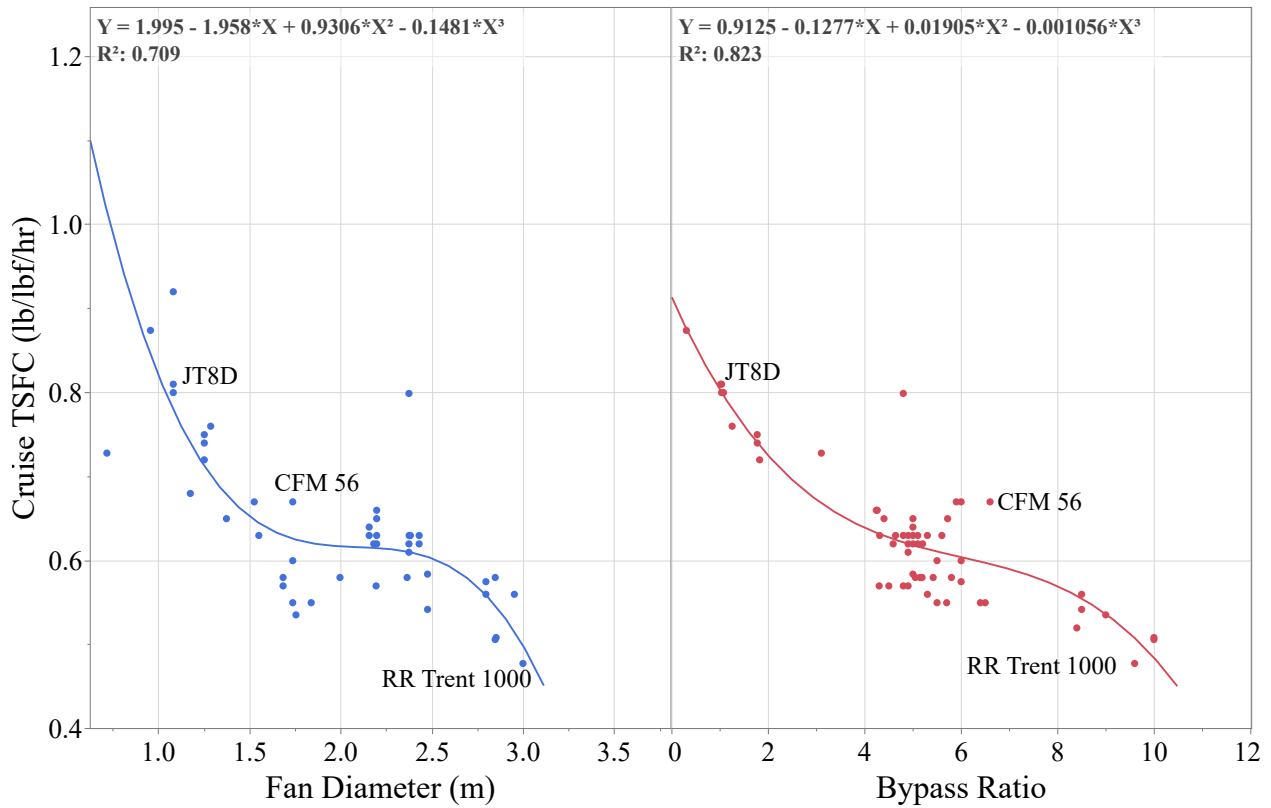


Fig. 20 Cruise thrust-specific fuel consumption versus engine diameter and bypass ratio, with well-known engines labeled to show generational differences.

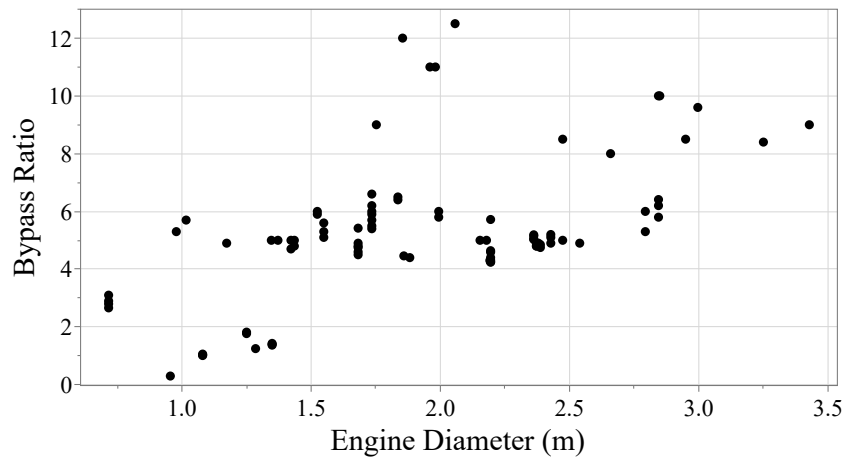


Fig. 21 Turbofan engine bypass ratio versus fan diameter.

cruise Mach numbers. Analysis of these diagrams reveals that aircraft generally cruise at a lower Mach number than the maximum operating limit. For example, while Boeing 757 and 767 both have a maximum operating cruise Mach number of 0.86, they typically cruise at Mach 0.8. This cruise Mach number of 0.8 was in fact found to be the mean of

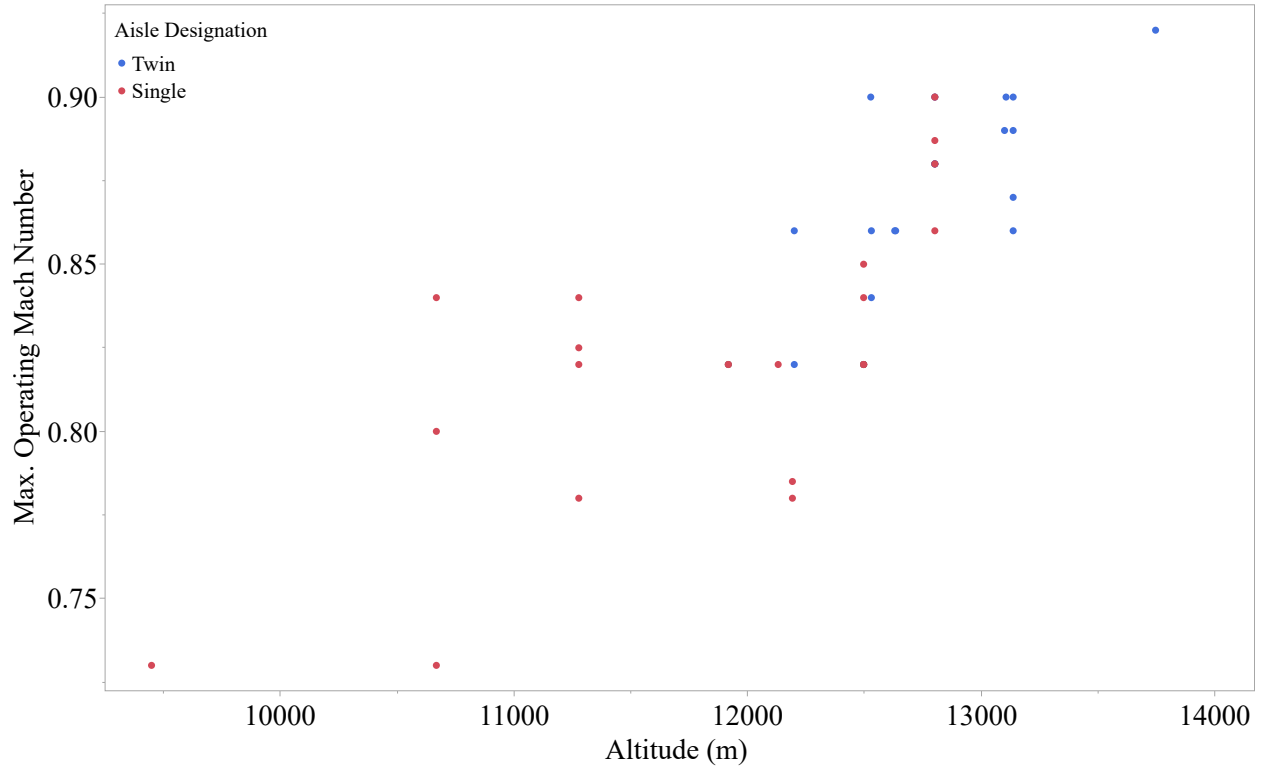


Fig. 22 Maximum operating Mach number versus cruise altitude for single-aisle (red) and twin-aisle (blue) aircraft.

the recorded values and was used for verification and lower asymptotic value projection in this study.

The cruise ambient to sea level temperature ratio θ is driven by the maximum cruise altitude, which is generally optimized for efficiency under FAA altitude certification limits and the structural pressurization load limits of the fuselage. As shown in Fig. 22, the historical data indicates that aircraft in the database operate at cruise altitudes ranging between 30,000 to 51,000 feet.

At these typical cruise altitudes, air temperature stabilizes around 392 °R. When normalized against sea-level temperature of 518 °R, this yields a temperature ratio of $\theta = 0.758$. Lastly, TSFC is also driven by the overall engine efficiency, which includes factors such as propulsive, combustion, and thermal efficiencies.

Achieving high levels of propulsive efficiency, such as those exceeding 0.8, is technically challenging and demands ongoing research into materials science, manufacturing, turbomachinery, heat exchangers, low-emission combustion systems, controls, and simulation capabilities. According to Singh et al. [50], a propulsive efficiency of higher than 0.8 can be reached with advanced turbofan engines and future technologies such as open-rotor (also called open fan or propfan) engines, as well as operating at lower cruise Mach numbers and using engines with higher bypass ratio.

As of 2012, the overall engine efficiency η_{tot} was estimated to be around 0.35, which remains well below the theoretical upper limit identified by Singh et al. [50]. The limitation on η_{tot} is primarily driven by the turbine entry

temperature (TET), overall pressure ratio (OPR), and combustion that ensures low nitrogen oxide (NOx) emission. Assuming the combustion is with hydrocarbon fuel, the TET for low NOx emission is limited between 2000 and 2100 Kelvin. Under these conditions, the practical upper limit for η_{tot} is 0.55. As seen in Eq. 8, increasing engine efficiency decreases fuel consumption. With a cruising Mach number of 0.8, cruise altitude of 35,000 ft, and η_{tot} of 0.55, the practical limit for cruise TSFC is 0.353 lb/lbf/hr.

If environmental impact and material limits are ignored, the theoretical limit of η_{tot} could reach as high as 0.65. This would assume stoichiometric combustion (2600 K), ideal component efficiencies, and overall pressure ratio higher than 80. With these conditions applied, the theoretical limit for TSFC at a cruise Mach of 0.8 and altitude of 35,000 feet is 0.299 lb/lbf/hr.

2. Future Projections of TSFC Trends

Practical and theoretical TSFC limits were derived using the aforementioned cruise conditions and overall efficiencies of 0.55 and 0.65 respectively. A NASA ARMD projection from 2019 reflects a conservative mid-term technology target, estimating a 50% improvement relative to the 2005 best-in-class engine. This engine is identified as the CFM56-7B used in the Boeing 737-800 with a cruise TSFC of 0.667 lb/lbf/hr. The result is a cruise TSFC of 0.334 lb/lbf/hr [51]. Figures 23a to 23c show S-curve projections of TSFC using these limits as lower asymptotes. Specifications for these S-curve models, including asymptotic values, inflection points, growth rates, and associated R^2 values, are detailed in Tab. 2.

Table 2 Specifications of S-curve models for turbofan cruise-specific fuel consumption given in Fig. 23.

Parameter	Practical Limit	Theoretical Limit	NASA 2019 [51]
Lower asymptote (lb/lbf/hr)	0.353	0.299	0.334
Upper asymptote (lb/lbf/hr)	1.000	1.000	1.000
Inflection point (year)	1981	1981	1981
Growth rate	-0.0632	-0.0556	-0.0595
R^2	0.5367	0.5264	0.5391

The inflection point year of 1981 was selected based on the interval of the most rapid TSFC improvement. Data on 83 unique engines was sourced from available TCDS cruise TSFC information. This inflection point maximized the R^2 values for the fitted S-curves, which is a goodness of fit metric, showing how much of the variation in TSFC is explained by the model. Due to the highly aggressive lower TSFC asymptote given by the theoretical limit, the associated $R^2 = 0.5264$ is the lowest of the methods. The practical limit S-curve yields an improved R^2 value of 0.5367, whereas the NASA limit shows the highest $R^2 = 0.5391$, using an intermediate lower asymptote. The differences in these R^2 values are very small, indicating that inflection year and growth rate dominate the S-curve model's ability to fit the data rather than the choice of asymptote. While the lower asymptote provided by the NASA projection creates a

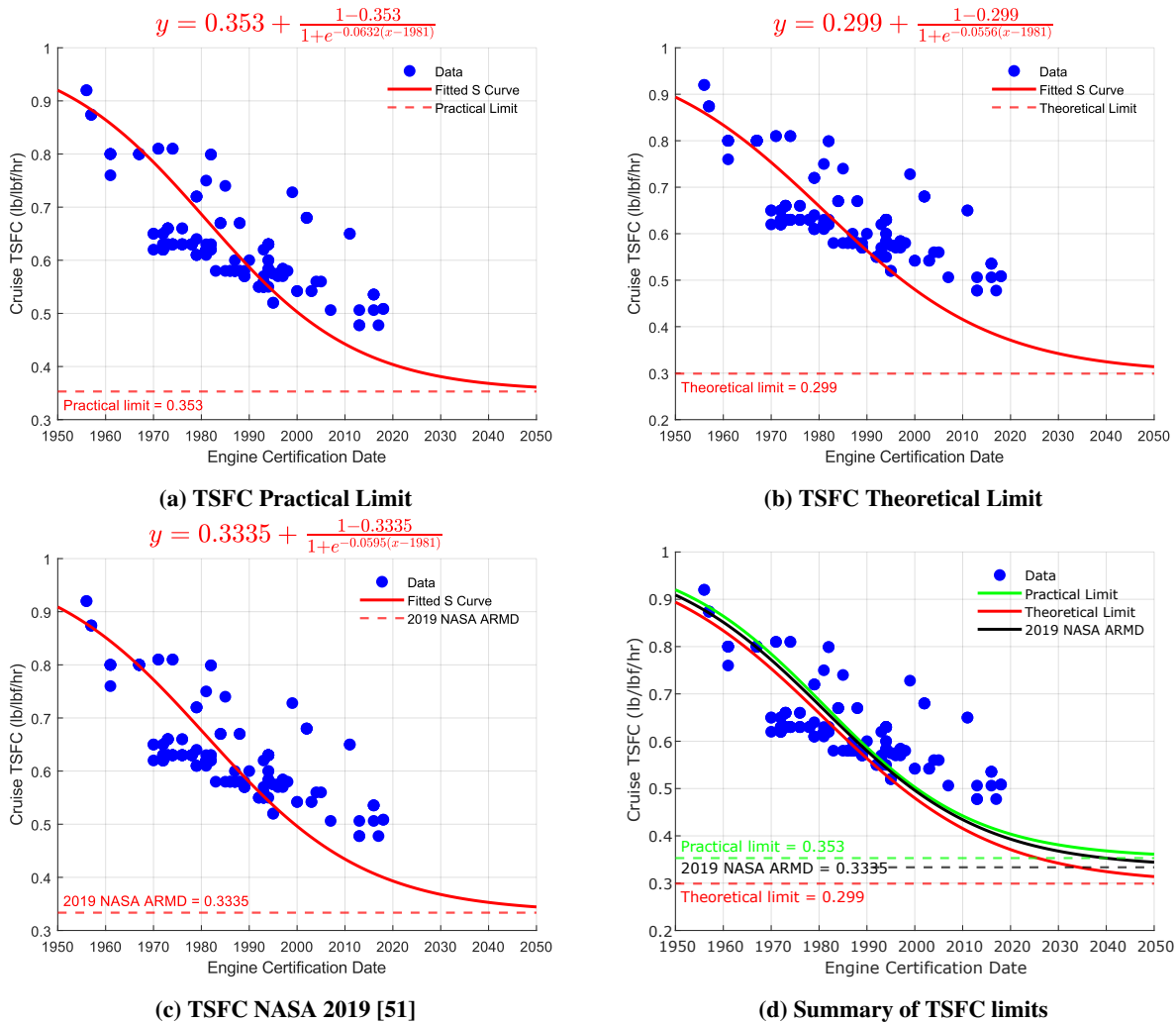


Fig. 23 Comparison of thrust-specific fuel consumption projections based on practical limits, theoretical limits, and NASA ARMD estimates.

curve with a marginally better fit, they are all comparable in explaining trends in TSFC improvements.

As mentioned previously, the cubic fit shown in Fig. 19 may initially appear to fit the TSFC data better than the methods presented here, showing an $R^2 = 0.668$. However the cubic fit is based entirely in statistics, ignoring the physical limitations which make the Sigmoid curve models robust. Although, the higher goodness of fit suggests that there may exist a model which better captures the trends explainable by the S-curves while preserving their robustness. Public TSFC data for modern engines—such as Pratt and Whitney’s geared turbofan series and the CFM LEAP family—are not available, as these engines remain under active development and their performance data are proprietary. However, both manufacturers claim 15-20% improvement in fuel consumption over previous generations [52, 53]. If these claims are accurate, the inclusion of TSFC data from these engines may be better captured by a revised two-phase model, in which a second period of rapid TSFC reduction begins around 2015, coinciding with the entry into service of

these advanced architectures.

While modern engines may suggest a renewed period of TSFC improvement, as noted above, emerging trends in the available data also indicate that high-bypass turbofans may be entering a maturity phase, where advancements yield progressively smaller TSFC improvements. One cause of this maturity could be the physical limitation on an engine's diameter. Underwing mounted engines are common in the commercial transport category, and an increase in their diameter presents a larger risk of nacelle ground-strikes in an emergency. If limited by mounting, future engines may not be able to increase fan size to realize gains in bypass ratio, a major factor in improving fuel economy. Research into further engine core minimization is ongoing, with NASA's Hybrid Thermally Efficient Core (HyTEC) and CFM's Revolutionary Innovation for Sustainable Engines (RISE) programs working to prove this [54, 55]. The HyTEC program, alongside its advancement of component level technology such as "advanced high pressure" turbomachinery and "combustion technologies," intends to demonstrate electrical power extraction from the gas turbine.

Electrified powertrain architectures could increase effective bypass ratios through propulsors which are mechanically disconnected from the gas turbine. NASA's Subsonic Single Aft eNginE (SUSAN) concept uses a turboelectric distributed propulsor architecture, which achieves an effective bypass ratio of over 20 [56]. Through distributed propulsion, ultra-high bypass ratios may be achieved without pushing the limit of underwing diameter limits.

The RISE program is also developing an open rotor engine, intended to increase the bypass ratio of turbofan-class engines to levels similar to turboprop engines. This work builds upon decades of open rotor research since the concept's inception in the 1980's [57], but differentiates itself by the removal of a second counter-rotating fan. Instead, it uses variable pitch stator blades which are quieter and lighter than previous designs, making the design more market competitive. Of course these engines are still limited by fan diameter, though without the need for a respectively large nacelle, may face a relaxed upper bound if mounted elsewhere than under the wing.

Achieving further TSFC improvement in conventional turbofans will result from core downsizing, however step changes in propulsive technology will likely result from further development of advanced engine architectures. Open-rotor and electrified configurations can alter the theoretical limit and shift TSFC projections to a new S-curve, establishing a new efficiency baseline for future engines.

D. Lift-to-Drag Ratio (L/D)

Lift-to-drag ratio (L/D) during cruise is a primary indicator of an aircraft's aerodynamic efficiency. The ability of an aircraft to produce the same amount of lift while incurring less drag, and therefore requiring less thrust—and consequently less energy, distinguishes it in a competitive market. As a result, L/D has generally increased over time, as manufacturers strive to design more efficient and commercially desirable aircraft for airlines. To conduct a meaningful analysis of L/D trends, access to direct L/D data is essential. However, reliable L/D data from primary sources like manufacturers or regulatory bodies, when publicly available, are extremely limited. Companies may maintain proprietary

databases containing such information, but public records from the FAA, EASA, or manufacturer data sheets rarely disclose these values, necessitating estimation methods based on other available parameters. Section III.D.1 below outlines the methods considered for estimating L/D using the data that were available from this study’s collection. Section III.D.2 discusses factors that influence historical trends in L/D, and Sec. III.D.3 projects potential future developments in L/D.

1. Challenges in L/D Data Collection and Estimation Methods

A significant challenge in analyzing L/D trends is the limited availability of publicly accessible, reliable cruise L/D data from primary sources, such as manufacturers or regulatory bodies. While companies may maintain proprietary databases with such information, neither public records from FAA, EASA, nor manufacturers’ data sheets typically disclose these values, necessitating estimation methods based on other available parameters.

This study applied three primary estimation methods:

- **Breguet Range Equation (BRE) Method:** Rearranged to solve for L/D using range, TSFC, cruise speed, and weight ratio:

$$\left. \frac{L}{D} \right|_{\text{Cruise}} = \frac{R * TSFC}{V_{\text{Cruise}} * \log \frac{1}{1 - \frac{W_{\text{Fuel}}}{W_{\text{MTOW}}}}} \quad (9)$$

- **Weight-to-Thrust Ratio Method:** Assumes a balance of lift with weight and drag with thrust during cruise (i.e., steady state cruise). Cruise weight is approximated from MTOW, adjusted using takeoff and climb fuel fractions, following Raymer’s formulation for transport aircraft [1]:

$$\left. \frac{L}{D} \right|_{\text{Cruise}} = \frac{W_{\text{Cruise}}}{T_{\text{Cruise}}} = \frac{W_{\text{MTOW}} * 0.995 * 0.985}{T_{\text{Cruise}}} \quad (10)$$

- **Mean Aerodynamic Chord (MAC) Method:** uses a regression model developed by Sforza [58], which relates L/D to the aspect ratio (AR) and Reynolds number at the mean aerodynamic chord (Re_{mac}):

$$\left. \frac{L}{D} \right|_{\text{Cruise}} = 0.321 * (AR^2 Re_{mac})^{3/16} (1 + 3.6AR^{-9/4})^{-1/2} \quad (11)$$

where

$$Re_{mac} \approx 7.093 \times 10^6 c_{mac} M [1 - 0.5(z/23,500)^{0.7}] \quad (12)$$

Equation (12) is applicable to Reynolds Numbers in the range 3×10^6 to 200×10^6 and altitudes between 0 and 50,000 feet mean sea level. This regression is obtained from basic configuration data for 14 airplanes as listed in Sforza [58].

Each method was applied using Aerobase data [10]. While individual sources in this database often included a

maximum operating Mach number for various aircraft, they generally lacked information on a typical cruise Mach number, which is essential for the MAC method. To address this, a median cruise Mach number was estimated and applied for aircraft missing this data.

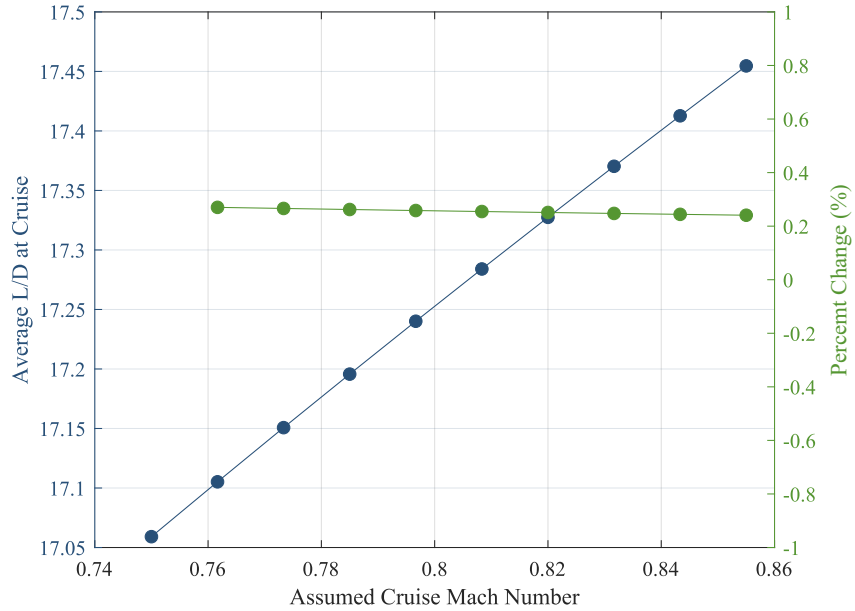


Fig. 24 Sensitivity of average database lift-to-drag ratio as a function of assumed cruise speed.

To ensure this assumption did not unduly influence the L/D estimates, a sensitivity analysis was conducted to examine how variations in the assumed cruise Mach number affected the average L/D . Cruise Mach was varied from 0.75 to 0.855, representing the observed range in the dataset. The results are shown in Fig. 24. This sensitivity analysis shows that the mean L/D increases with assumed Mach Number, which is consistent with the direct relationship between the two in the MAC method presented in Eq. 12. Although the effect of assuming a Mach number for unknown values does result in changes to the MAC method L/D trends, the effect is on the order of 0.4, as seen in Fig. 24. In Fig. 25, it can be seen that a shift of this magnitude in the MAC L/D curves is inconsequential when compared to the absolute scale ($L/D \sim 16-20$) of the data. Historically, cruise Mach numbers did increase as designers optimized transonic performance, particularly to manage drag divergence effects. However, subsonic cruise speeds have since reached a near-constant level due to physical constraints around the speed of sound and fuel efficiency considerations. Thus, for this analysis, a median cruise Mach number of 0.8 was selected to ensure consistent comparisons without introducing significant bias.

With this assumption in place, sufficient data was available to apply the MAC method meaningfully across the dataset to predict the cruise L/D trends. Fig. 25 presents L/D estimates derived using three methods across the historical database, showing distinct trends and variability for both single-aisle and twin-aisle aircraft, with 90% confidence ellipses to indicate variability in each category.

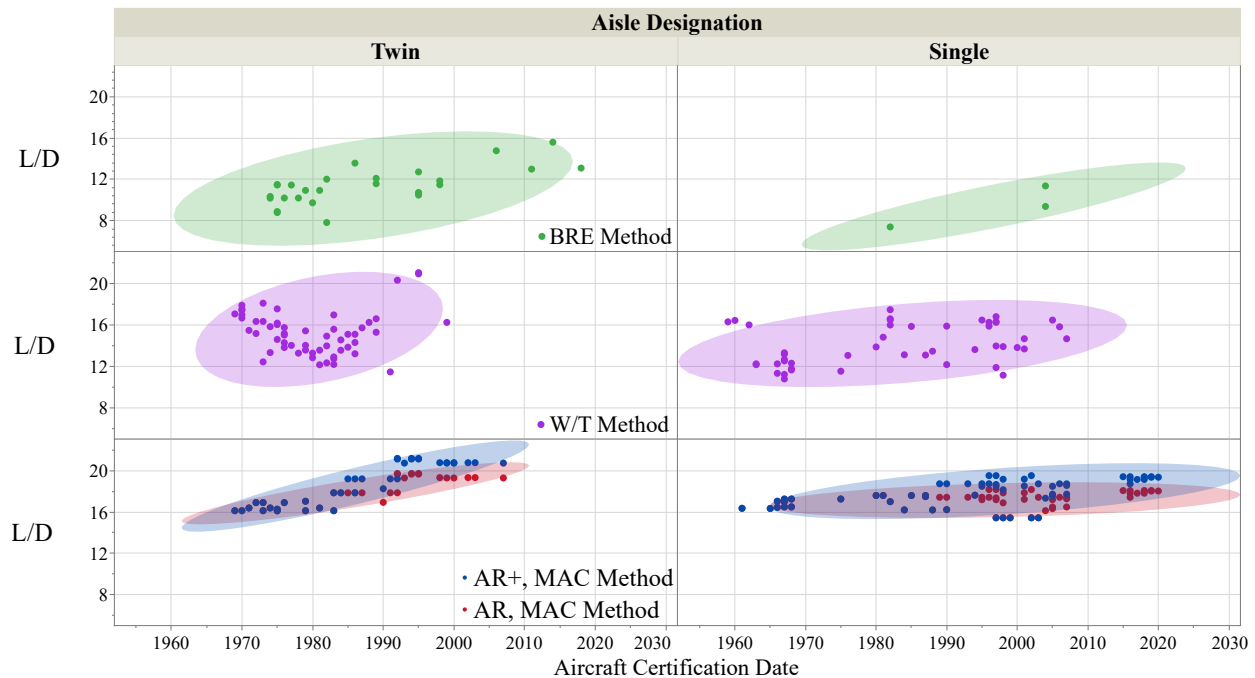


Fig. 25 Historical trends in lift-to-drag ratio as calculated using multiple methods, grouped by aisle, with 90% confidence ellipses to illustrate variability. The legend differentiates between lift-to-drag (L/D) calculations based on whether the aspect ratio was adjusted (+ 20%) for the presence of wingtip devices, indicated as ‘AR+’ for the adjusted calculation and ‘AR’ for the unadjusted version. This distinction is only relevant to the MAC method.

The BRE method does not have sufficient data to draw conclusions in the single-aisle category. This is due to the lack of reliable cruise TSFC data in literature, which are required by this method. Predictions using BRE consistently fall below practical L/D values. This discrepancy likely arises from methodological assumptions regarding fuel weight and range. Since W_{Fuel} values from the database may represent maximum fuel capacity—including reserve fuel for diversion and holding—this could yield an overestimate of fuel weight relative to the actual mission fuel, resulting in lower L/D values. Additionally, typical commercial mission ranges reported in the data sources exclude reserve missions, causing a further imbalance.

The weight-to-thrust method has broader data coverage since it relies on more commonly available parameters in TCDS and APMs. However, these predictions also suffer from being unrealistic, showing a wide L/D range (12 to 24). This variability likely results from fuel fraction estimations used to approximate cruise weight. Unlike real flight conditions, where weight decreases continuously due to fuel burn, this method applies fixed weight fractions that cannot account for the dynamic nature of weight reduction during cruise. Therefore, while this method might be useful for capturing broader trends, its limitations in accuracy make it unsuitable for accurate historical L/D trend analysis.

Finally, the MAC method predicts L/D estimates within an intuitive range and with greater consistency across aircraft types. Its reliance on aspect ratio allows for a more accurate assessment of the effect of wing configuration changes over time, including the adoption of wingtip devices. Applying an effective aspect ratio increase of approximately 20% to

account for wingtip devices (following Raymer's model [1]) aligns well with observed improvements in aerodynamic efficiency for single-aisle aircraft, where wingspan limitations have necessitated design optimizations. The resulting effect of the improved L/D for aircraft with wingtip devices, using this method, is reflected in the trends shown in Fig. 25, with color coding to distinguish configurations.

In summary, the MAC method emerges as the most reliable estimator for historical L/D trends, providing consistency and sensitivity to aerodynamic configurations over time. For future analysis, the W/T method could potentially be refined through more detailed fuel burn modeling. Meanwhile, the BRE method's limitations emphasize the importance of accurate mission-specific data inputs for estimating L/D, as general fuel and range assumptions can substantially skew results.

2. Factors Influencing L/D Trends

While L/D has shown improvement over time, examining the trends of other aerodynamic parameters provides more information on the reasoning behind this phenomenon, contextualizing the evolution of L/D. Figure 26 illustrates the historical trends of key aerodynamic parameters, grouped by aisle count, with 90% confidence ellipses. MTOW and wing loading (W/S) are shown to remain largely constant over time, along with wing area trends. This suggests that improvements in L/D arise primarily from optimizing the shape and configuration of the wing within a fixed area. In both aisle aircraft categories, L/D gains appear more modest without the consideration of wingtip devices, reinforcing that these devices are a primary driver of L/D improvement after the 1980s. However, twin-aisle aircraft do show a general increase in wingspan, which may account for the greater increase in aspect ratio compared to single aisle aircraft, as well as the more dramatic increase in L/D when wingtip device effects are neglected.

With primary aerodynamic benefits resulting from the inclusion of wingtip devices, further analysis is performed. Figure 27 charts the different devices employed by aircraft across decades. Marker color distinguishes major manufacturers (with Douglas and McDonnell Douglas treated as a single entity), and the spacing between markers in the same wingtip category in the same year has been added solely for visual clarity and does not represent any statistical trends. Wingtip devices are recorded for the original model as built by the manufacturer (i.e., retrofits and aftermarket upgrades are excluded). Wingtip devices were first introduced in the early to mid 1980s and subsequently saw widespread adoption by major manufacturers, and after 2000 it became standard practice to include wingtip devices on aircraft. Early applications in the 1980s and 1990s typically employed basic wingtip fences or canted tips. In the 2000s and 2010s, designs evolved to include blended wingtips (referred to as "Sharklets" by Airbus) or raked wingtips by Boeing. Most recently, a newer scimitar design, which resembles a large blended wingtip fence, has been introduced by Boeing. The Boeing 777X (still being certified at the time of this article's publication), employs folding wingtips. This new technology allows the wingspan of the aircraft to fit within wingspan limitations when on the ground, while offering the aerodynamic benefits of a larger aspect ratio in flight.

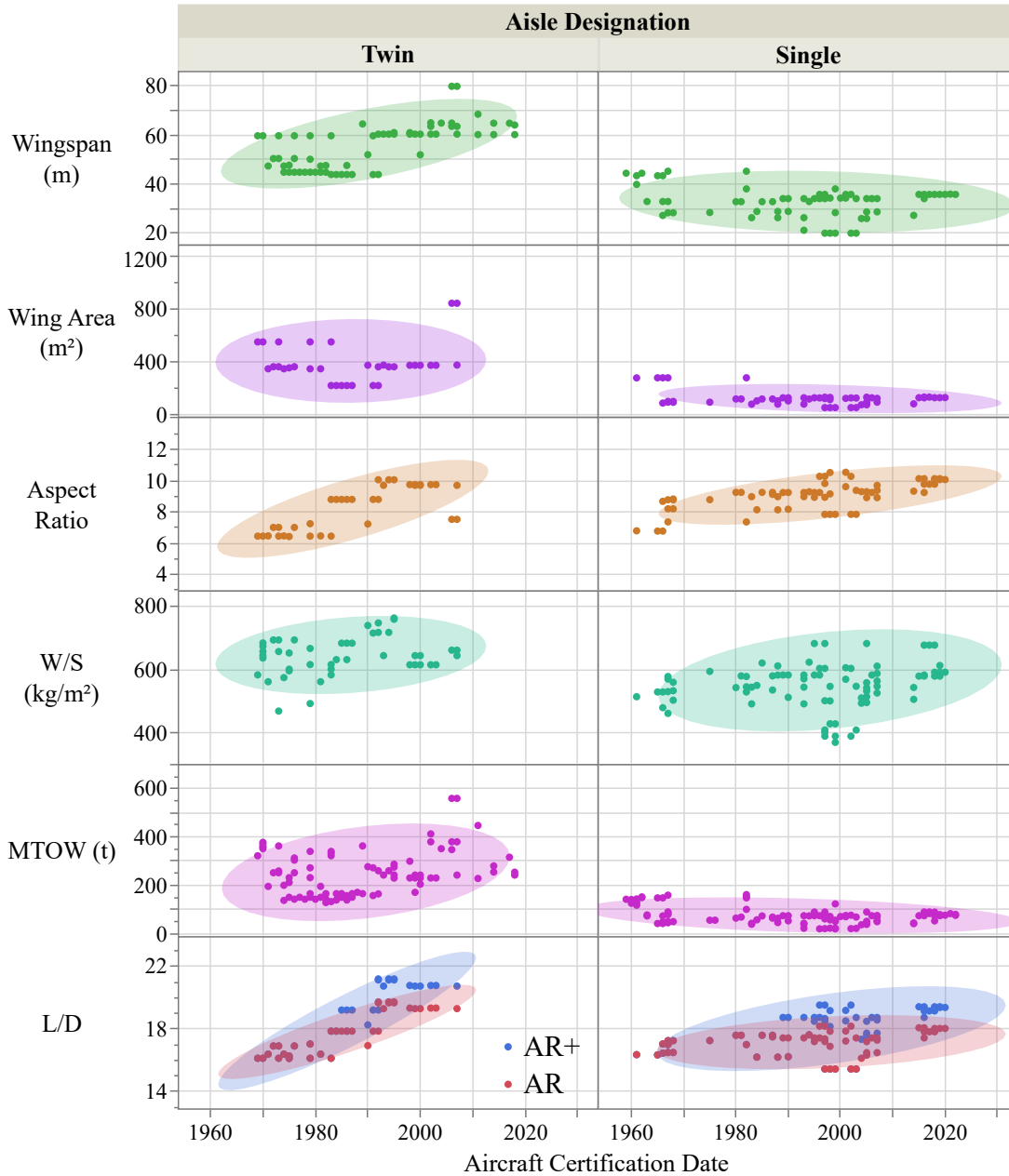


Fig. 26 Evolution of key aerodynamic parameters, grouped by aisle count, with 90% confidence ellipses showing trends over time. The legend differentiates between lift-to-drag (L/D) calculations based on whether the aspect ratio was adjusted (+ 20%) for the presence of wingtip devices, indicated as ‘AR+’ for the adjusted calculation and ‘AR’ for the unadjusted version. The MAC method was used to calculate L/D in this figure.

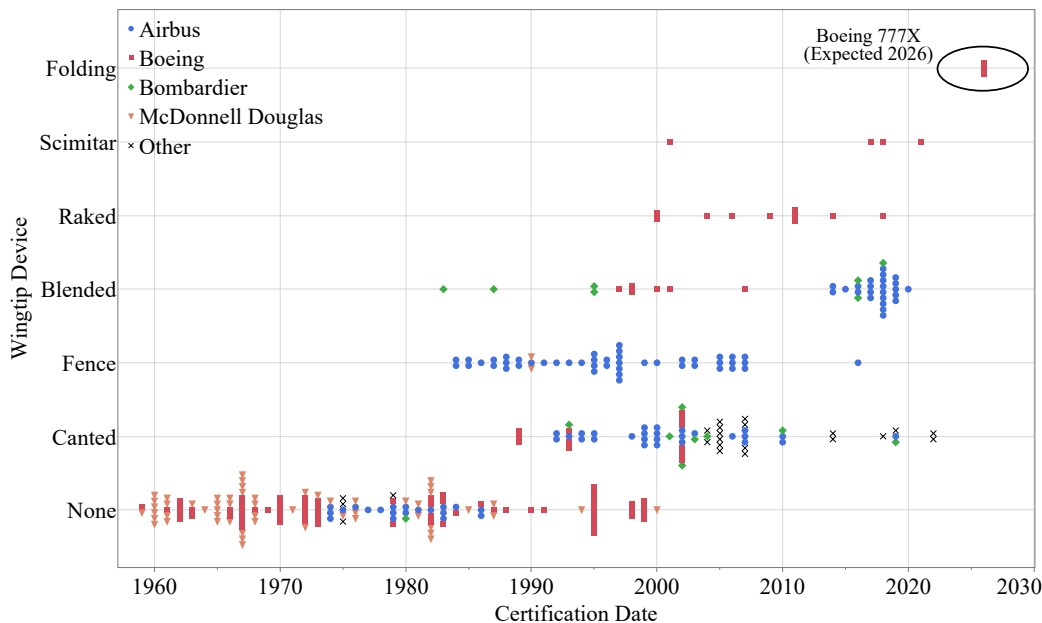


Fig. 27 Wingtip devices used on aircraft over time, where marker color and shape determine the manufacturer of the aircraft. The spacing between markers in the same wingtip category in the same year has been added solely for visual clarity and does not represent any statistical trends. Douglas and McDonnell Douglas are treated as a single entity. Annotation added for the Boeing 777X, expected certification in 2026.

As previously mentioned, it is more efficient to design an aircraft with a larger aspect ratio rather achieve similar aerodynamic benefits with wingtip devices [1]. Despite this, wingtip devices are continuously implemented and improved. Several factors may explain this apparent trade-off. Foremost among them is the fact that aircraft are rarely designed from a clean sheet, most designs evolve from previous generations. Incremental design evolution often limits the feasibility of major geometric changes, and adding wingtip devices is an inexpensive and quick avenue for improving aerodynamics relative to overhauling the entire aircraft. It is for this same reason that wingtip devices have been used to retrofit older generation aircraft. Wingtips have also been used to make up for shortcomings of other subsystems. For example, during the development of the A340, IAE failed to deliver the ultra-high-bypass “SuperFan,” leading Airbus to adopt a newer blended wingtip (over their previous fence design) along with extending the wingspan to make up for the fuel benefits that would have been gained with the new engine [59] [60].

Wingtip devices may also be used to accommodate regulatory restrictions. While advancements in structural technology may enable the inclusion of a wider wingspan on a newer generation aircraft, a larger wingspan may push an aircraft into a larger Airplane Design Group (ADG), defined by limits on wingspan and tail height. The term “ADG” was established by the FAA in 1989 [61], where airport infrastructure constraints, such as taxiway widths and wingtip clearances, are defined for each ADG. There have been several amendments to the document since its release, however the wingspan and tail height limits have remained unchanged [62, 63]. An analogous regulation exists outside

of the United States. The ICAO uses Aerodrome Reference Code (ARC), which has wingspan limits in its groups identical to those defined by ADG [64]. The first edition of this document, published in 1951, includes a more basic classification, but does not categorize aircraft into groups according to wingspan or tail height [65]. A second edition was not published until 1995, after the original FAA advisory circular in 1989. This temporal gap suggests that the FAA was the first to codify wingspan-based grouping, later incorporated into ICAO standards. Wingspan limitations for each design group, along with representative aircraft, are provided in Tab. 3.

ADG	ARC	Wingspan Limit [63, 64]	Tail Height Limit [63]	Aircraft
III	C	36m (118ft)	13.7m (45ft)	A320, 737
IV	D	52m (171ft)	18.3m (60ft)	A300, A310, 707, 767 *
V	E	65m (214ft)	20.1m (66ft)	A330, A340, A350, 777, early 747s
VI	F	80m (262ft)	24.4m (80ft)	A380, 747-800

Table 3 Geometric limits for airplane design group/aerodrome reference codes with prototypical aircraft in each group. Note that ICAO does not have explicit limits for tail height set.

An aircraft in a larger design group may be less competitive from an airline’s perspective as some airports’ infrastructure may not be able to accommodate larger design group aircraft. Airports also typically charge higher fees for larger aircraft. While these fees usually scale with gross weight and not design group, the two are closely related. Additionally, existing infrastructure may prevent aircraft in larger groups from operating out of certain airports.

Figure 28 shows the evolution over time of the ADG limiter for different aircraft. The limit percentage on the y-axis is calculated from $\max(b/b_{\text{limit}}, h/h_{\text{limit}})$, where b is wingspan and h is tail height, while the limit varies for each group, as shown in Tab. 3. Color distinguishes whether the limiting factor is tail height or wingspan, while shape denotes whether the aircraft employs wingtip devices. Three clear patterns emerge. First, wingspan is typically the primary limiting factor in determining an aircraft’s design group.. This is intuitive as vertical tails are sized to meet engine-inoperative yaw control requirements, and increasing tail height alone does not necessarily improve aerodynamic performance. Second, in recent decades, more aircraft than before are near the limit of their ADG. This trend supports the hypothesis that designs progressively increase their aspect ratio higher (also supported by Fig. 26) until constrained by external limits. The collection of aircraft near the 100% limit line suggests that this restriction is regulatory as opposed to structural, for example. Third, after the year 2000, all aircraft above 90% of their ADG limit on wingspan employ wingtip devices, suggesting that wingtip devices are used to increase aerodynamic efficiency when further increases in wingspan are not possible.

Interestingly, as seen in Fig. 26, wingspan for twin-aisle aircraft increases generally over time, which appears to contradict the hypothesis presented above. However, ADG trends show a large halt in the production of group IV aircraft around 1990, where group V aircraft start to become more common. This paradigm shift from group IV to

*Most group IV (D) aircraft were certified prior to the formalization of the grouping system.

group V, both of which contain primarily twin-aisle aircraft, may explain why twin-aisle aircraft are seen to grow in wingspan over time while single aisle are not. The absence of formal ADG classifications prior to 1989 may explain the transitional shift observed. The replacement of legacy twin-aisle aircraft, which would have been in group IV, with the next generation, which would be in group V, may have been set in motion before this practice was codified. If legacy single aisle aircraft in group III were being replaced with more advanced aircraft that still fell within group III, manufacturers would have had continued incentive to remain within this group to preserve fleet compatibility.

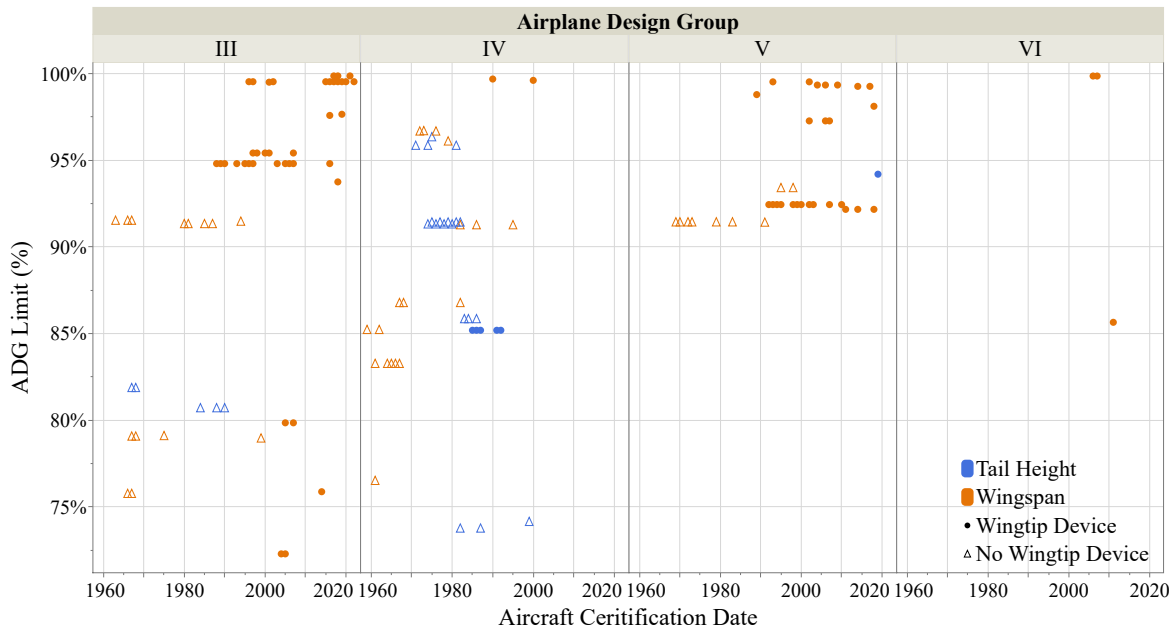


Fig. 28 Airplane design group limiting factor as a percentage of the maximum allowable value for a given ADG. Color distinguishes whether the limiting factor was the aircraft’s tail height or wingspan, while shape designates which aircraft employ wingtip devices and which do not.

3. Future Projection of L/D Trends

Optimizing L/D involves a complex multidisciplinary design process, balancing aerodynamic shaping with structural and operational constraints. Efforts to overcome the aerodynamic efficiency limitations of traditional tube-wing designs have led to the exploration of unconventional aircraft configurations, predominately the truss-braced wing (TBW) and hybrid (sometimes called blended) wing body (HWB, BWB) geometries.

The TBW has historical roots, dating back to the H.D. 31, a high-aspect ratio prototype that first flew in 1953. It was later developed into the H.D. 321, which flew in 1955 with an aspect ratio of 20.2 [66, 67]. The H.D. aircraft cruised at approximately Mach 0.22, considerably slower than modern requirements. Modern transonic truss-braced wing (TTBW) studies began in 2007 when NASA announced research opportunities under the subsonic fixed wing (SFW)

project [68]. Boeing's subsonic ultra green aircraft research (SUGAR) team was awarded the contract in 2008 [69] and in 2011 published a Phase I report [70], detailing analyses conducted on five aircraft concepts, one of which was the "SUGAR High," a TTBW concept that showed promise in increasing cruise L/D to approximately 26, compared to contemporary values in the 18-22 range. While this represents a significant improvement in L/D , the calculation was performed under the assumption that the concept would include technologies such as low interference nacelles and struts/braces, as well as riblets applied to the fuselage and aft wing surfaces. Although the SUGAR High concept has an aspect ratio of approximately 23, some of the improvement in L/D may be due to the inclusion of these assumed surface enhancements. SFW studies continued through the 2010s into the 2020s. The work done on the Sugar High concept was foundational to Boeing's award of a funded Space Act Agreement to construct a TTBW aircraft under the sustainable flight demonstrator project [69, 71]. The full-scale flight demonstrator, eventually designated the X-66A [72], represented a significant step toward widespread adoption of higher L/D technology. As of May 2025, the project has been put "on ice" by Boeing [73], which could delay the implementation timeline of TBW technology.

Primitive HWB concepts were introduced as early as the 1920s, involving airfoil-shaped fuselages and lifting-body geometries [74]. Flying wing concepts were not uncommon in throughout the 20th century [75], and eventually, in 1989, the Spirit B-2 bomber saw its first flight. Interest in commercial HWB applications increased in the 1990s, and preliminary studies were performed throughout the decade [76]. The first major industry involvement came in 2007 when the X-48B first flew [77]. Boeing designed the X-48 series, scale model HWB aircraft with wingspans of approximately 20 feet, under NASA's environmentally responsible aviation (ERA) program. While L/D data for the X-48 aircraft are not publicly reported, the ERA project final report on the conceptual design of subscale test vehicles shows cruise L/D in the approximate range of 22 to 24 for several HWB configurations. These values are contextualized by a comparison to advanced tube and wing configurations, which saw cruise L/D in the 20 to 23 range. Both the HWB and advanced tube and wing concepts assumed the use of riblets, a hybrid laminar flow control system, and included raked wingtips [78]. Around the same time, Boeing's SUGAR team also developed the SUGAR Ray HWB concept in parallel with the SUGAR High. The SUGAR concepts showed similar promise in L/D , with the SUGAR Ray reported to have an L/D of approximately 26.5 in cruise [70], also calculated assuming surface enhancements. Recently, the HWB concept has moved beyond conceptual and subscale validation. JetZero, a startup focused on the design of HWB aircraft, was contracted by the United States Air Force to fly a full scale HWB demonstrator, called the "Z4," by 2027 [79, 80]. JetZero has since certified a 12.5% scale prototype for flight testing, in addition to announcing a partnership with Delta Airlines to focus on solutions to operational challenges with HWB aircraft.

While early-stage conceptual development is common in all sectors of the aerospace industry, the scale and diversity of recent partnerships suggest a consensus on the next stage of commercial aircraft evolution. The data in this study have shown that a principal driver of improving aerodynamic efficiency has come from the implementation of wingtip devices, a relatively mild change in geometry compared to the TTBW and HWB. The data showing new aircraft approaching

the regulatory limits on their wingspans suggests that further refinement of the tube and wing architecture may offer diminishing returns. Supporting technological advancements are being developed in parallel and are expected to mature alongside new aircraft configurations, however the SUGAR and ERA studies have shown the aerodynamic benefits of architectural changes under the same subsystem assumptions. Technologies such as riblets, laminar flow control, and folding wingtips improve the aerodynamics of any aircraft, however a step change in L/D will come from the widespread implementation of aircraft architectures with higher potential than that of the tube and wing.

IV. Conclusions and Future Work

This work provides a comprehensive examination of historical trends and future projections of key performance parameters (KPPs) in commercial turbofan aircraft design. Drawing on an extensive database of over 400 commercial aircraft and 200 engines from authoritative sources such as FAA and EASA Type Certificate Data Sheets and manufacturers' specifications, this research offers a transparent and reliable foundation for KPP analysis. The study examined four critical KPPs: operational empty weight to maximum takeoff weight ratio (OEW/MTOW), thrust-to-weight ratio (T/W), thrust specific fuel consumption (TSFC), and lift-to-drag ratio (L/D).

The analysis of OEW/MTOW underscores the complexity of its relationship with structural efficiency. Historical data reveals that this ratio is significantly influenced by market-driven demands such as range and aircraft size rather than exclusively by technological improvements in structural materials. Although materials like composites have demonstrably contributed to weight savings in specific cases, such as the A350 compared to the A330, their broad impact on OEW/MTOW trends remains nuanced and mission-dependent. As alternatives like hydrogen and electrified propulsion systems emerge, their unique weight characteristics result in OEW/MTOW values that deviate significantly from those of conventional aircraft, potentially representing a jump to new S-curves in technological development.

Examination of the T/W ratio highlights its primary dependence on operational performance requirements rather than purely on propulsion technology advancements. Incremental increases observed historically, particularly in single-aisle aircraft, reflect evolving regulatory and operational demands, such as noise abatement and shorter takeoff distances. Future T/W developments are expected to stabilize barring significant shifts in design philosophy or mission specifications. However, unconventional designs—such as blended-wing bodies and hydrogen-powered aircraft—may exhibit distinctly different T/W characteristics due to their unique structural and aerodynamic attributes.

The analysis of TSFC revealed a clear downward trend over the past decades, strongly correlating with technological progress in engine efficiency. Bypass ratio was shown to have a large impact on TSFC, historically increased through a combination of core downsizing and engine up-sizing. Applying S-curve modeling, the study projected that TSFC is approaching its practical lower limits with current turbofan technology, based on physical considerations such as overall engine efficiency and environmental constraints. Substantial further reductions in TSFC may require adopting disruptive propulsion technologies such as ultra-high bypass ratio engines, open rotors, or electrified systems.

The analysis of L/D identified the mean aerodynamic chord-based approach as the most reliable for capturing aerodynamic trends. L/D has improved modestly over time, primarily due to aerodynamic refinements within the constraints of conventional tube-and-wing configurations. A large contributor to aerodynamic refinement was the usage of wingtip devices, which have continued to evolve since their adoption in the 1980s. However, gains are increasingly challenging as designs approach practical (regulatory and structural) aerodynamic efficiency limits. Future improvements in L/D may require unconventional configurations, such as hybrid wing bodies or truss-braced wings, which offer potential for substantial aerodynamic advancements. Coupled interactions between step changes in airframe and engine technology may accelerate the improvement in overall aircraft efficiency.

A major contribution of this research is the public release of the data used in the various KPP analyses. The FAST Aerobase is available for researchers and students to draw additional conclusions and expand upon this work [10]. The Aerobase laid the foundation for the development of the Future Aircraft Sizing Tool (FAST), which integrates historical KPP trends to streamline initial aircraft design. As an open-source tool, FAST facilitates rapid exploration of design spaces with minimal inputs, leveraging a combination of physics-based and data-driven models. By embedding these historical KPP insights, this work provides aircraft designers and researchers with a robust, transparent resource for informed decision-making in early design stages. In addition to their practical applications, the data-driven insights presented here offer educational value. While many discussions of aircraft performance trends address historical data in general terms, this study delineates the underlying physical drivers that shape these trends, allowing a clearer understanding of the nuanced interactions among KPPs, mission requirements, and technology advances.

Collectively, these findings supply credible baselines against which emerging propulsion and airframe concepts can be judged, and they offer educators a concrete exposition of the physical mechanisms shaping KPP trends. Future work should (i) incorporate data for geared-fan and open-rotor engines as they enter service, (ii) extend the database to regional turboprop and business-jet sectors, and (iii) couple airframe and engine S-curves to assess fully integrated aero-propulsive benefits.

Funding Sources

This work is sponsored by the NASA Aeronautics Research Mission Directorate and Electrified Powertrain Flight Demonstration project, “Development of a Parametrically Driven Electrified Aircraft Design and Optimization Tool,” WO-0238. Karin Bozak serves as NASA’s Technical Monitor.

Acknowledgments

The authors would like to thank Ralph Jansen, Amy Chicatelli, Andrew Meade, Karin Bozak, and Gaudy Bezos O’Connor from NASA’s Electrified Powertrain Flight Demonstration project for supporting this work and providing valuable technical input and feedback throughout the duration of the project. AI-based editing assistance (Writefull) was

used for grammar and language refinement during manuscript preparation. The tool did not contribute to the research design, analysis, or interpretation of results.

References

- [1] Raymer, D. P., *Aircraft design: A conceptual approach*, 4th ed., AIAA education series, American Institute of Aeronautics and Astronautics, Reston, Va., 2006. URL <http://www.loc.gov/catdir/toc/ecip068/2006004706.html>.
- [2] Roskam, J., and Lan, C., *Airplane Aerodynamics and Performance*, Airplane design and analysis, Roskam Aviation and Engineering, 1997.
- [3] Torenbeek, E., *Synthesis of Subsonic Airplane Design*, Delft University Press, Delft, 1982.
- [4] Martinez-Val, R., Perez, E., and Palacin, J., “Historical Perspective of Air Transport Productivity and Efficiency,” *43rd AIAA Aerospace Sciences Meeting and Exhibit*, American Institute of Aeronautics and Astronautics, 2005. <https://doi.org/10.2514/6.2005-121>.
- [5] Lee, J. J., Lukachko, S. P., Waitz, I. A., and Schafer, A., “Historical and Future Trends in Aircraft Performance, Cost, and Emissions,” *Annual Review of Energy and the Environment*, Vol. 26, No. 1, 2001, p. 167–200. <https://doi.org/10.1146/annurev.energy.26.1.167>.
- [6] Ballal, D. R., and Zelina, J., “Progress in Aeroengine Technology (1939–2003),” *Journal of Aircraft*, Vol. 41, No. 1, 2004, p. 43–50. <https://doi.org/10.2514/1.562>, URL <http://dx.doi.org/10.2514/1.562>.
- [7] Martinez-Val, R., Palacin, J. F., and Perez, E., “The evolution of jet airliners explained through the range equation,” *Proceedings of the Institution of Mechanical Engineers, Part G: Journal of Aerospace Engineering*, Vol. 222, No. 6, 2008, p. 915–919. <https://doi.org/10.1243/09544100jaero338>.
- [8] Martinez-Val, R., and Perez, E., “Aeronautics and astronautics: Recent progress and future trends,” *Proceedings of the Institution of Mechanical Engineers, Part C: Journal of Mechanical Engineering Science*, Vol. 223, No. 12, 2009, p. 2767–2820. <https://doi.org/10.1243/09544062jmes1546>.
- [9] Babikian, R., Lukachko, S. P., and Waitz, I. A., “The historical fuel efficiency characteristics of regional aircraft from technological, operational, and cost perspectives,” *Journal of Air Transport Management*, Vol. 8, No. 6, 2002, pp. 389–400. [https://doi.org/https://doi.org/10.1016/S0969-6997\(02\)00020-0](https://doi.org/https://doi.org/10.1016/S0969-6997(02)00020-0).
- [10] IDEAS Laboratory, “FAST Aerobase,” , 2024. URL <https://github.com/ideas-um/FAST/tree/main/%2BDatabasePkg>.
- [11] Mokotoff, P., Arnson, M., Wang, Y.-C., and Cinar, G., “FAST: A Future Aircraft Sizing Tool for Conventional and Electrified Aircraft Design,” *AIAA SCITECH 2025 Forum*, American Institute of Aeronautics and Astronautics, 2025. <https://doi.org/10.2514/6.2025-2374>.

- [12] Duffy, K. P., and Jansen, R., “Partially Turboelectric and Hybrid Electric Aircraft Drive Key Performance Parameters,” *2018 AIAA/IEEE Electric Aircraft Technologies Symposium*, American Institute of Aeronautics and Astronautics, 2018. <https://doi.org/10.2514/6.2018-5023>, URL <http://dx.doi.org/10.2514/6.2018-5023>.
- [13] Jansen, R., Duffy, K. P., and Brown, G., “Partially Turboelectric Aircraft Drive Key Performance Parameters,” *53rd AIAA/SAE/ASEE Joint Propulsion Conference*, American Institute of Aeronautics and Astronautics, 2017. <https://doi.org/10.2514/6.2017-4702>.
- [14] Jansen, R., Brown, G. V., Felder, J. L., and Duffy, K. P., “Turboelectric Aircraft Drive Key Performance Parameters and Functional Requirements,” *51st AIAA/SAE/ASEE Joint Propulsion Conference*, American Institute of Aeronautics and Astronautics, 2015. <https://doi.org/10.2514/6.2015-3890>.
- [15] Pastra, C. L., Hall, C., Cinar, G., Gladin, J., and Mavris, D. N., “Specific Power and Efficiency Projections of Electric Machines and Circuit Protection Exploration for Aircraft Applications,” *2022 IEEE Transportation Electrification Conference amp; Expo (ITEC)*, IEEE, 2022, p. 766–771. <https://doi.org/10.1109/itec53557.2022.9813927>, URL <http://dx.doi.org/10.1109/itec53557.2022.9813927>.
- [16] Hall, C., Pastra, C. L., Burrell, A., Gladin, J., and Mavris, D. N., “Projecting Power Converter Specific Power Through 2050 for Aerospace Applications,” *2022 IEEE Transportation Electrification Conference amp; Expo (ITEC)*, IEEE, 2022, p. 760–765. <https://doi.org/10.1109/itec53557.2022.9813991>, URL <http://dx.doi.org/10.1109/itec53557.2022.9813991>.
- [17] Tiede, B., O’Meara, C., and Jansen, R., “Battery Key Performance Projections based on Historical Trends and Chemistries,” *2022 IEEE Transportation Electrification Conference amp; Expo (ITEC)*, IEEE, 2022, p. 754–759. <https://doi.org/10.1109/itec53557.2022.9814008>, URL <http://dx.doi.org/10.1109/itec53557.2022.9814008>.
- [18] Roux, E., *Turbofan and Turbojet Engines: Database Handbook*, Éditions Élodie Roux, 2007.
- [19] Roux, E., *Turboshaft, Turboprop and Propfan: Database Handbook*, Éditions Élodie Roux, 2011.
- [20] *Janes All the World’s Aircraft: In service 2022-2023*, Jane’s group UK limited., 2022. URL https://books.google.com/books?id=bw_yzgEACAAJ.
- [21] Administration, F. A., “Aircraft Characteristics Data,” , 2023. Data retrieved from FAA, https://www.faa.gov/airports/engineering/aircraft_char_database/data.
- [22] Eurocontrol, “Aircraft Performance Database,” , n.d. URL <https://contentzone.eurocontrol.int/aircraftperformance/default.aspx>.
- [23] Jenkinson, L., Simpkin, P., and Rhodes, D., “Civil Jet Aircraft Design Data Sets,” , 2001. URL <https://booksite.elsevier.com/9780340741528/appendices/default.htm>.
- [24] Arnson, M. G., Aljaber, R., and Cinar, G., “Predicting Aircraft Design Parameters Using Gaussian Process Regressions on Historical Data,” *AIAA SCITECH 2025 Forum*, American Institute of Aeronautics and Astronautics, 2025. <https://doi.org/10.2514/6.2025-1287>.

- [25] Rashid, M., Sarkar, J., and Phuyal, S., “Visualizing Bivariate Statistics Using Ellipses Over a Scatter Plot,” *Journal of Probability and Statistical Science*, Vol. 20, No. 1, 2022, p. 150–165. <https://doi.org/10.37119/jpss2022.v20i1.584>.
- [26] JMP, “Confidence Ellipse,” <https://www.jmp.com/support/help/en/18.0/index.shtml#page/jmp/ellipse.shtml>, 2024. Accessed: 2024-09-05.
- [27] Epstein, A. H., “Aeropropulsion for Commercial Aviation in the Twenty-First Century and Research Directions Needed,” *AIAA Journal*, Vol. 52, No. 5, 2014, p. 901–911. <https://doi.org/10.2514/1.j052713>.
- [28] Torenbeek, E., *Advanced Aircraft Design: Conceptual Design, Analysis and Optimization of Subsonic Civil Airplanes*, Wiley, 2013. <https://doi.org/10.1002/9781118568101>.
- [29] Wolleswinkel, R. E., de Vries, R., Hoogreef, M., and Vos, R., “A New Perspective on Battery-Electric Aviation, Part I: Reassessment of Achievable Range,” *AIAA SCITECH 2024 Forum*, American Institute of Aeronautics and Astronautics, 2024. <https://doi.org/10.2514/6.2024-1489>.
- [30] CLEVELAND, F., “Size effects in conventional aircraft design,” *2nd Aircraft Design and Operations Meeting*, American Institute of Aeronautics and Astronautics, 1970. URL <http://dx.doi.org/10.2514/6.1970-940>.
- [31] Aerospace Technology Institute, “Sustainable Cabin Design,” Tech. Rep. FZO-AIR-POS-0039, FlyZero Project, 2022. URL <https://www.ati.org.uk/wp-content/uploads/2022/03/FZO-AIR-POS-0039-Sustainable-Cabin-Design.pdf>, accessed April 2025.
- [32] Dubois, T., “Aircraft Passenger Seat Design Gets Smarter,” *Aviation Week Network*, 2020. URL <https://aviationweek.com/mro/interiors-connectivity/aircraft-passenger-seat-design-gets-smarter>, accessed April 2025.
- [33] Fuchte, J. C., Nagel, B., and Gollnick, V., “Weight and Fuel saving Potential Through Changed Cabin and Fuselage Design,” *2013 Aviation Technology, Integration, and Operations Conference*, American Institute of Aeronautics and Astronautics, 2013. <https://doi.org/10.2514/6.2013-4305>, URL <http://dx.doi.org/10.2514/6.2013-4305>.
- [34] Expliseat, “TiSeat 2X for A320 Family,” , 2025. URL https://expliseat.com/wp-content/uploads/2025/04/250402_Expliseat-Flyer_TiSeat-2-X-A320_Flyers-_preview_single.pdf, product brochure, accessed April 2025.
- [35] “14 CFR Part 36: Noise Standards – Aircraft Type and Airworthiness Certification,” <https://www.ecfr.gov/current/title-14/chapter-I/subchapter-C/part-36>, 2025. U.S. Code of Federal Regulations, effective 2025.
- [36] International Civil Aviation Organization, “Environmental Technical Manual (ETM) Volume I: Procedures for the Noise Certification of Aircraft,” https://www.icao.int/environmental-protection/Documents/SGAR_2018_ETM_Vol_I.pdf, 2018. Doc 9501, Volume I.
- [37] Federal Aviation Administration, “Advisory Circular AC 91-53A: Noise Abatement Departure Profiles,” https://www.faa.gov/documentLibrary/media/Advisory_Circular/AC_91-53A.pdf, 1993. Provides acceptable criteria for noise abatement departure profiles for subsonic turbojet-powered aircraft over 75,000 lbs.

- [38] Lee, C. H., Salit, M. S., and Hassan, M. R., "A Review of the Flammability Factors of Kenaf and Allied Fibre Reinforced Polymer Composites," *Advances in Materials Science and Engineering*, Vol. 2014, 2014, p. 1–8. <https://doi.org/10.1155/2014/514036>, URL <http://dx.doi.org/10.1155/2014/514036>.
- [39] Qian, J., and Alonso, J., "Structural Optimization of Blended Wing Body Transport Aircraft With Buckling Constraints," *AIAA AVIATION 2021 FORUM*, American Institute of Aeronautics and Astronautics, 2021. <https://doi.org/10.2514/6.2021-3022>.
- [40] Scholz, D., "The blended wing body (BWB) aircraft configuration," *Kolloquium: 75 Jahre Flugzeugbaustudium in Hamburg (1935–2010)*, 2010.
- [41] Xisto, C., and Lundbladh, A., "Design and performance of liquid hydrogen fueled aircraft for year 2050 EIS," *33rd Congress of the international council of the aeronautical sciences*, 2022.
- [42] Antcliff, K. R., Guynn, M. D., Marien, T., Wells, D. P., Schneider, S. J., and Tong, M. J., "Mission Analysis and Aircraft Sizing of a Hybrid-Electric Regional Aircraft," *54th AIAA Aerospace Sciences Meeting*, American Institute of Aeronautics and Astronautics, 2016. <https://doi.org/10.2514/6.2016-1028>, URL <http://dx.doi.org/10.2514/6.2016-1028>.
- [43] Mukhopadhaya, J., and Graver, B., "Performance analysis of regional electric aircraft," *International Council of Clean Transportation white paper*, 2022.
- [44] Gladin, J. C., *Performance Assessment of Electrified Aircraft*, Cambridge University Press, 2022, p. 256–293. <https://doi.org/10.1017/9781108297684.010>.
- [45] Mattingly, J. D., Heiser, W. H., and Pratt, D. T., *Aircraft Engine Design, Second Edition*, American Institute of Aeronautics and Astronautics, 2002. <https://doi.org/10.2514/4.861444>, URL <http://dx.doi.org/10.2514/4.861444>.
- [46] Kellari, D., Crawley, E. F., and Cameron, B. G., "Influence of Technology Trends on Future Aircraft Architecture," *Journal of Aircraft*, Vol. 54, No. 6, 2017, p. 2213–2227. <https://doi.org/10.2514/1.c034266>.
- [47] Kumar, P., and Khalid, A., "Blended Wing Body Propulsion System Design," *International Journal of Aviation, Aeronautics, and Aerospace*, 2017. <https://doi.org/10.15394/ijaaa.2017.1187>, URL <http://dx.doi.org/10.15394/ijaaa.2017.1187>.
- [48] NASA Glenn Research Center, "Specific Fuel Consumption (SFC)," <https://www.grc.nasa.gov/www/k-12/airplane/sfc.html>, 2021. Accessed: 2024-11-05.
- [49] National Academies of Sciences, Engineering, and Medicine, *Commercial Aircraft Propulsion and Energy Systems Research: Reducing Global Carbon Emissions*, National Academies Press, 2016. <https://doi.org/10.17226/23490>, URL <http://dx.doi.org/10.17226/23490>.
- [50] Singh, R., Ameyugo, G., and Noppel, F., *Jet engine design drivers: past, present and future*, Elsevier, 2012, p. 56–82. <https://doi.org/10.1533/9780857096098.1.56>, URL <http://dx.doi.org/10.1533/9780857096098.1.56>.
- [51] National Aeronautics and Space Administration, "NASA Aeronautics Strategic Implementation Plan: 2019 Update," <http://www.nasa.gov>, 2019. NASA Aeronautics Research Mission Directorate.

- [52] CFM International, “LEAP Engines Lower Fuel and Emissions While Enhancing Efficiency,” <https://www.cfmaeroengines.com/press-articles/cfm-delivering-leap-engines-that-lower-fuel-nozzle-maintenance-burden>, 2023. Accessed April 2025.
- [53] Pratt & Whitney, “GTF Engines – Commercial Engines Overview,” <https://www.prattwhitney.com/en/products/commercial-engines/gtf#Fast%20Facts>, 2024. Accessed April 2025.
- [54] Nerone, A. L., Haglage, J. M., Nakley, L. M., and Tornabene, R., “NASA Hybrid Thermally Efficient Core (HyTEC) Project Overview,” *34th Congress of the International Council of the Aeronautical Sciences (ICAS)*, ICAS, Florence, Italy, 2024. Presented September 9–13, 2024.
- [55] CFM International, “CFM RISE Program: Revolutionary Innovation for Sustainable Engines,” Tech. rep., CFM International, 2021. URL <https://www.cfmaeroengines.com/press-articles/cfm-launches-revolutionary-rise-program-to-develop-future-sustainable-aviation-technologies>, whitepaper detailing CFM’s open fan technology roadmap, fuel efficiency goals, and integration strategy.
- [56] Chapman, J. W., Kratz, J. L., Dever, T., Mirhashemi, A., Heersema, N., and Jansen, R., “SUSAN Concept Vehicle Power and Propulsion System Study,” *AIAA SCITECH 2023 Forum*, American Institute of Aeronautics and Astronautics, 2023. <https://doi.org/10.2514/6.2023-1749>.
- [57] GE Aircraft Engines, “Full Scale Technology Demonstration of a Modern Counterrotating Unducted Fan Engine Concept: Design Report,” Tech. Rep. NASA CR-180867, National Aeronautics and Space Administration (NASA), NASA Lewis Research Center, 1987. Prepared under NASA Contract NAS3-24210 by the GE36 Project Department, Cincinnati, Ohio.
- [58] Sforza, P. M., “Direct Calculation of Zero-Lift Drag Coefficients and (L/D)_{max} in Subsonic Cruise,” *Journal of Aircraft*, Vol. 57, No. 6, 2020, pp. 1224–1228. <https://doi.org/10.2514/1.C035717>.
- [59] Gunston, B., *Airbus*, J H Haynes, Yeovil, England, 2009, p. 201.
- [60] Norris, G., and Wagner, M., *Airbus A340 and A330*, Motorbooks International, Minneapolis, MN, 2001, p. 31.
- [61] Federal Aviation Administration, “Advisory Circular 150/5300-13: Airport Design,” , Sep. 1989. U.S. Department of Transportation.
- [62] Federal Aviation Administration, “Advisory Circular 150/5300-13A: Airport Design,” , Feb. 2014. U.S. Department of Transportation.
- [63] Federal Aviation Administration, “Advisory Circular 150/5300-13B: Airport Design,” , Aug. 2024. U.S. Department of Transportation.
- [64] International Civil Aviation Organization, *Annex 14 - Aerodromes, Volume I - Aerodrome Design and Operations*, 9th ed., International Civil Aviation Organization, 2022.
- [65] International Civil Aviation Organization, *Annex 14 - Aerodromes*, 1st ed., International Civil Aviation Organization, 1951.

- [66] Bridgman, L. (ed.), *Jane's All the World's Aircraft*, Jane's, 1958. URL <https://archive.org/details/janesallworldsai0000na>, accessed via Internet Archive on 2025-04-11.
- [67] Warwick, G., "Gallery: A Timeline Of The Truss-Braced Wing," *Aviation Week Network*, 2020. URL <https://aviationweek.com/TBWTimeline>, accessed: 2025-04-11.
- [68] "Amendment 2 to NASA Research Announcement ROA-2008: Appendix A.2 Subsonic Fixed Wing (SFW)," Tech. Rep. NNH08ZEA001N-SSF1, National Aeronautics and Space Administration (NASA), Washington, DC, Mar. 2008. URL <https://www.federalgrants.com/Opportunity-NNH08ZEA001N-SUP3-15072.html>, focus on advanced concept studies for subsonic commercial transport aircraft entering service in the 2030–2035 timeframe.
- [69] Wells, D. P., Gatlin, G. M., June, J. C., and Marien, T. V., "NASA Transonic Truss-Braced Wing Studies," *33rd Congress of the International Council of the Aeronautical Sciences (ICAS)*, ICAS, 2024. URL https://www.icas.org/ICAS_ARCHIVE/ICAS2024/data/papers/ICAS2024_0108_paper.pdf.
- [70] Bradley, M. K., and Droney, C. K., "Subsonic Ultra Green Aircraft Research: Phase I Final Report," Tech. Rep. NASA/CR–2011-216847, NASA, Huntington Beach, California, 2011. URL <https://ntrs.nasa.gov/citations/20110014687>.
- [71] JEC Composites, "Boeing selected for NASA Sustainable Flight Demonstrator award," , 2023. URL <https://www.jeccomposites.com/news/spotted-by-jec/boeing-selected-for-nasa-sustainable-flight-demonstrator-award/>, accessed: 2025-04-11.
- [72] O'Shea, C. A., "Next Generation Experimental Aircraft Becomes NASA's Newest X-Plane," , Jun. 2023. URL <https://www.nasa.gov/news-release/next-generation-experimental-aircraft-becomes-nasas-newest-x-plane/>, nASA Release 23-068, Accessed: 2025-04-11.
- [73] Norris, G., "Boeing Puts X-66 On Ice But Will Continue Thin Wing Studies," *Aviation Week & Space Technology*, 2025. URL <https://aviationweek.com/aerospace/emerging-technologies/boeing-puts-x-66-ice-will-continue-thin-wing-studies>.
- [74] Brar, R., "Design of a Blended Wing Body Aircraft," Master's thesis, San José State University, Dec. 2014. Advisor: Dr. Nikos Mourtos.
- [75] States, U., and Larrimer, B., *Beyond Tube-and-Wing: The X-48 Blended Wing-Body and NASA's Quest to Reshape Future Transport Aircraft*, NASA aeronautics book series, National Aeronautics and Space Administration, 2020. URL <https://books.google.com/books?id=kYTIzQEACAAJ>.
- [76] Chambers, J., *Innovation in Flight: Research of the NASA Langley Research Center on Revolutionary Advanced Concepts for Aeronautics: NASA History Series*, CreateSpace Independent Publishing Platform, 2007. URL https://books.google.com/books?id=u_9kngEACAAJ.
- [77] Creech, G., "X-48 Research: All Good Things Must Come to an End," , Apr. 2013. URL <https://www.nasa.gov/centers/armstrong/news/NewsReleases/2013/13-13.html>, accessed: 2025-04-11.

- [78] Bonet, J. T., Schellenger, H. G., Rawdon, B. K., Elmer, K. R., Wakayama, S. R., Brown, D. L., and Guo, Y., “Environmentally Responsible Aviation (ERA) Project - N+2 Advanced Vehicle Concepts Study and Conceptual Design of Subscale Test Vehicle (STV): Final Report,” Tech. Rep. NASA/CR—2011-216519, NASA, Dryden Flight Research Center, Edwards, California, 2011. URL <https://ntrs.nasa.gov/citations/20110011635>.
- [79] JetZero, “JetZero Accelerates Fuel-Efficient Airliner Development with \$235 Million Air Force Award,” , Aug. 2023. URL <https://www.prnewswire.com/news-releases/jetzero-accelerates-fuel-efficient-airliner-development-with-235-million-air-force-award-301903000.html>, accessed: 2025-04-10.
- [80] Department of the Air Force, “DAF selects JetZero to develop blended wing body aircraft prototype,” , Aug. 2023. URL <https://www.af.mil/News/Article-Display/Article/3494520/daf-selects-jetzero-to-develop-blended-wing-body-aircraft-prototype>, accessed: 2025-04-10.